

CHAPTER ONE

Introduction And Basic Concepts

1.1 Introduction

The basic principles of atomic and molecular spectra have not changed since the advent of quantum mechanics in 1925. However, with the use of lasers in the last 20 years, there has been a remarkable improvement in both the intensity and resolution of the spectral light source. With increased light intensity we can now probe highly excited states of atoms and molecules and with increased spectral resolution we can observe more structural details [1].

Nowadays, by spectroscopy, we usually mean experimental charting of the energy levels structure of physical systems. For that purpose, the transition processes, spontaneous or induced, between different energy states are studied and spectroscopy therefore normally means analysis of various types of radiation electromagnetic or particle emission [2].

So we can define Spectroscopy by the branch of science dealing with the study of interaction of electromagnetic radiation with matter. The most important consequence of such interaction is that is absorbed or emitted by the matter in discrete amounts called quanta [3].

The important assumption in spectroscopic measurements is that Beer's law relationship applied between a change in spectrometer response and that concentration of analyte material present in a sample specimen [4].

1.2 Absorption and emission of radiation

If an atom or a molecule absorbs a photon its own energy is enhanced and on the contrary if a photon is emitted by an atom or a molecule it becomes less energetic [3].

1.2.1 Absorption

When electromagnetic radiation passes through matter, a variety of phenomenon may occur some of these are as follows:

If the photons of radiation possess the appropriate energies, they may be absorbed by the matter and result in electronic transitions, rotational changes, vibrational changes or combination of these. After absorption, atoms and molecules become excited. They give out energy quickly either by losing energy in the form of heat or by re-emitting electromagnetic radiation.

It is not necessary that the radiation passing through the matter may be absorbed completely. The portion of the electromagnetic radiation that passes into matter, instead of being absorbed, may undergo scattering or reflection or may be re emitted at the same or different wavelength.

When electromagnetic radiation is neither absorbed nor scattered, it may undergo changes in orientation or polarization [3].

Let us now assume that the atom is initially lying in level 1 if this is the ground level, the atom will remain in this level unless some external stimulus is applied to it. We shall assume, then, that an electromagnetic wave of frequency $\nu = \nu_0$ is incident on the material. In this case there is a finite probability that the atom will be raised to level 2. Figure (1.1) Show the energy difference $E_2 - E_1$ required by the atom to undergo the transition is obtained from the energy of the incident electromagnetic wave. This is the absorption process [5].

The equation shown below defines the rate of absorption as:

$$dN_2/dt = - W_{12}N_1$$

where, N_1 is the number of atoms per unit volume, which at a give time, are all at energy level E_1 . N_2 is the number of atoms per unit volume in a specific material which is at energy level E_2 , W_{12} is the probability of absorption transition, which is also another coefficient by Einstein.

in case of absorption also, we can write

$$W_{12} = \Phi C_{12}$$

Where, C_{12} is the cross section of absorption, which depends on the type of transition and Φ is the flux density of photons [6].

1.2.2 Spontaneous Emission:

To describe the phenomenon of spontaneous emission, let us consider two energy levels, 1 and 2, of some atom or molecule of a given material, their energies being E_1 and E_2 ($E_1 < E_2$) as in figure (1-1). the two levels could be any two out of the infinite set of levels possessed by the atom [5].

Let us call the energy level E_1 as 'normal level' or 'ground level'

Consider that the atom of the material is at energy level E_2 . The atom at this level is more unstable as compared to that at the ground level. Naturally, there is a tendency for the atom to come back to or 'decay' into ground level. So when decay occurs, the atom releases some amount of energy. When this energy is released in the form of electromagnetic waves, we call it the process of radiation or "Spontaneous Emission" of energy [6].

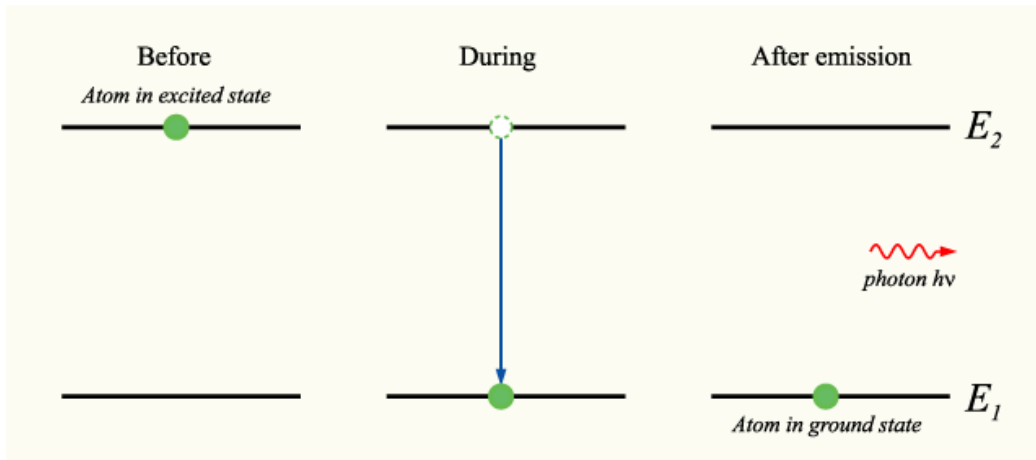


Figure (1.1) : The process of Spontaneous Emission

1.2.3 Stimulated Emission:

Einstein in 1917 first introduced the concept of stimulated or induced emission of radiation by atomic systems. He showed that in order to describe completely the interaction of matter and radiation, it is necessary to include that process in which an excited atom may be induced, by the presence of radiation, to emit a photon, and thereby decay to a lower energy state [7].

Let us now suppose that the atom is found initially in level 2 and that an electromagnetic wave of frequency $\nu = \nu_0$ is incident on the material (figure 1.2). Since this wave has the same frequency as the atomic frequency, there is a finite probability that this wave will force the atom to undergo the transition $2 \longrightarrow 1$. In this case the energy difference $E_2 - E_1$ is delivered in the form of an electromagnetic wave that adds to the incident one. This is the phenomenon of stimulated emission [5]. This is the origin of Light Amplification by Stimulated Emission of Radiation or (LASER).

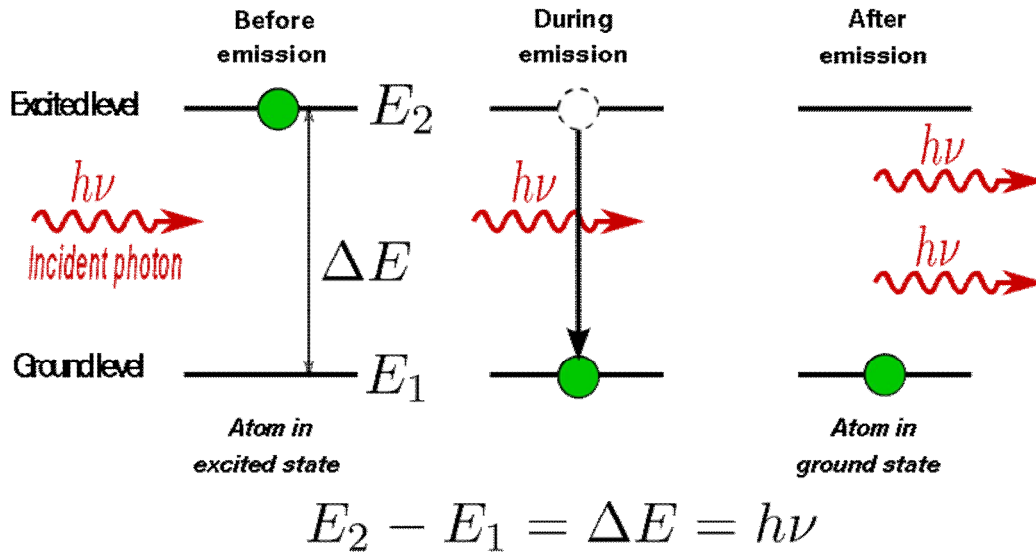


Figure (1.2) : The process of Stimulated Emission

1.3 Fundamental of Lasers

A laser (an acronym for light amplification by stimulated emission of radiation) is a device that produces and amplifies an intense beam of highly coherent, highly directional light. The original proposal of extending the maser (microwave amplification by stimulated emission of radiation) idea to the infrared or visible region of the electromagnetic (EM) spectrum, thus giving a laser, was however first made in 1960 by Maiman using a flash-pumped rod of ruby with polished ends (ruby laser) after a proposal in 1958 by Townes and Schawlow [8].

The laser makes use of processes that increase or amplify light signals after those signals have been generated by other means. These process include (1) stimulated emission, a natural effect that was deduced by consideration relating to thermodynamic equilibrium, and (2) Optical feedback (present in most laser) that is usually provided by mirrors. Thus, in it's simplest form, a laser consists a gain or amplifying medium (where

stimulated emission occurs), and a set of mirrors to feed the light back in to the amplifier for continued growth of the developing beam [9].

1.3.1 Properties of Laser Beams

Laser radiation shows an extremely high degree of monochromaticity, coherence, directionality and brightness as compared to other noncoherent light sources.

A. Monochromaticity:

The monochromaticity of laser radiation is a unique property of laser light, results from the circumstance that light oscillation sets in at one resonance frequency of the optical cavity, and owing to the balance between gain and loss in CW operation the line width $\Delta\nu_L$ of the oscillating mode is ultimately limited by quantum noise.

B. Coherence:

The coherence of laser radiation refers to the time period Δt in which the phase undergoes random changes, and the coherence length is a measure of the propagation distance over which the beam stays coherent [10].

C. Directionality:

The directionality of the laser beam is due to the fact that the gain medium is placed inside an open optical resonator.

D. Brightness:

The brightness of laser radiation is closely related to the directionality and stems from the capability of a laser oscillator to emit a high optical power in a small solid angle of space [8].

1.4 Laser in Spectroscopy

The impact of lasers on spectroscopy can hardly be overestimated. Laser represent intense light source with spectral energy densities which may exceed those of incoherent sources by several orders of magnitude. Furthermore, because of their extremely small bandwidth, single – mode

lasers allow a spectral resolution which far exceeds that of conventional spectrometers. Many experiments which could not be done before the application of lasers, because of lack of intensity or insufficient resolution, are readily performed with lasers.

Now several thousands of laser lines are known which span the whole spectral range from the vacuum – ultraviolet to the far-infrared region. Of particular interest are the continuously tunable lasers which may in many cases replace wavelength – selecting elements, such as spectrometers or interferometers [11].

Laser spectroscopy has many types of technique such as :

1.4.1 Laser Raman Spectroscopy

Raman spectroscopy is of considerable interest for quantitative measurements on wide number of processes. Further, important flame species such as O₂, N₂ and H₂ [2].

Raman spectroscopy is used to determine molecular structures and compositions of organic and inorganic materials. Materials in the solid and liquid are easily examined; even gas samples can be handled under special conditions. Normally the minimum sample requirements are on the order of tenths of a gram.

In the basic Raman experiment, a sample is illuminated by a high-energy monochromatic light source (typically from a laser). Some of the incident photons collide with molecules in the sample and are scattered in all directions with unchanged energy; that is, most collisions are elastic with the frequency of the scattered light (ν) being the same as that of the original light (ν_0). The effect is known as Rayleigh scattering. However, a second type of scattering can also occur and is known as the Raman effect.

In laser Raman scattering, the molecule can either accept energy from the incident laser being scattered, thus exciting the molecule into higher vibrational energy states (Stokes lines), or give up energy to the incident photons, causing the molecule to return to its ground vibrational state (anti-Stokes lines), showing in figure (1.3) The difference between the incident laser and the Raman scattered radiations produces the vibrational spectrum of interest.

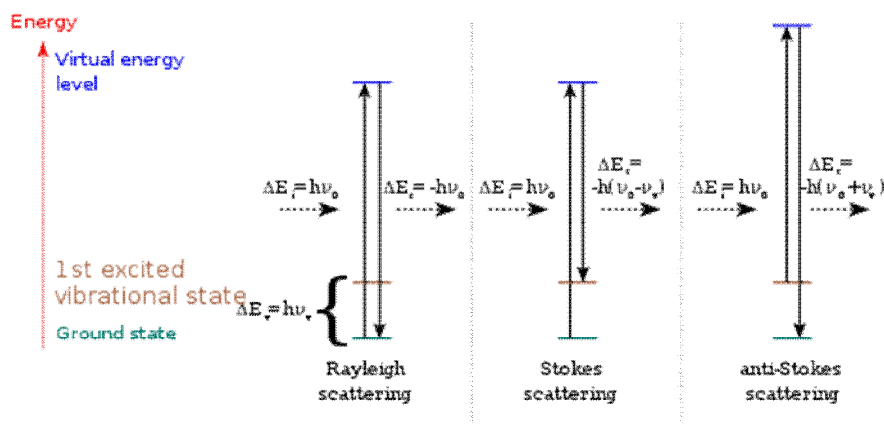


Figure (1.3) : Schematic diagram showing the The different possibilities of light scattering: Rayleigh scattering, Stokes scattering and anti-Stokes scattering.

Raman spectroscopy determining the wavelengths of Raman-shifted light can characterize minerals, detect trace amounts of organic substances and identify biological substances such as proteins, DNA, amino acids and plant pigments. The method often is used in medicine, for tasks that range from analyzing genes to detecting microbes.

The basic process of Raman spectrometry. The mineral sample to be studied is illuminated by a laser beam. Scattered light is collected by the spectrometer. A filter removes any light that is the same color as the laser beam, letting only the light that has changed color (Raman-shifted light)

pass through. The diffraction grating separates the light by color (wavelength). The different wavelengths are collected by a charged couple device (CCD) camera. A computer creates a graph showing the intensity of light at each wavelength figure (1.4).

A planetary Raman spectrometer would press a probe against a sample, or perhaps plunge a fiber-optic cable into the soil, then fire the laser repeatedly as the probe scanned the sample. A special filter would remove scattered light that had not changed color. Raman-shifted light would pass through the filter, then pass through a grating and bend according to wavelength. The light would hit an electronic camera. A computer would convert the data collected by the camera into graphs showing the "spectra" or wavelengths of the Raman-shifted light. Organic substances and minerals can be identified by the "peaks" they create at certain wavelengths on these graphs.

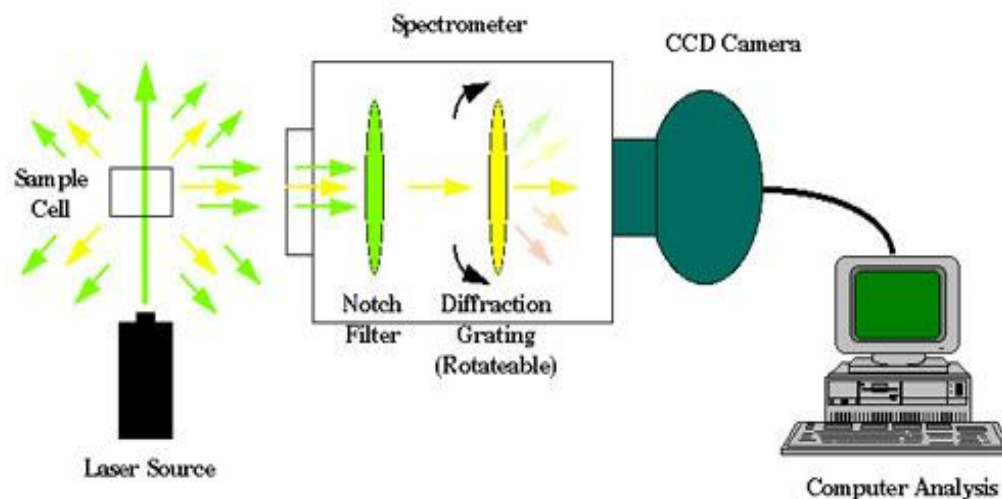


Figure (1.4) Schematic diagram of laser Raman spectrometer.

1.4.2.Laser induced fluorescence (LIF) .

Laser induced fluorescence (LIF) is the optical emission from atoms or molecules that have been excited to higher energy levels by absorption of electromagnetic radiation. The main advantage of fluorescence detection compared to absorption measurements is the greater sensitivity achievable because the fluorescence signal has a very low background . In the case of resonant excited molecules, Laser induced fluorescence (LIF) provides selective analyte excitation, thus avoiding interferences . Laser induced fluorescence (LIF) can be profitably applied to study the electronic structure of molecules and to perform quantitative measurements of analyte concentrations.

The development of investigation tools for identification, mapping and evaluation of natural or pollutant components is a key action in environment protection, ecosystem safeguard and life sustaining. Remote operation, prompt response, real-time analysis, and large area scanning are the demands and the skills requested in order to supply and establish guidelines for conservation, management and remediation actions.

In addition, Laser induced fluorescence (LIF) can be very effective in significant measurements of the bio-optical parameters in vegetation and/or natural waters. This laser technique has proved Qualitative (flow visualization) and analytical applications include measurements of gas-phase concentrations in the atmosphere [12], in experimental fluid mechanics to measure the concentration of a scalar species within a fluid [13], and in determining the density of a certain atomic level in the plasma directly from the absorption coefficient [14].

Figure (1.5) shows the typical PLIF setup consists of a laser an arrangement of lenses to form a sheet, fluorescent medium, collection

optics and a detector. The light from the laser, illuminates the medium, which then fluoresces. This signal is captured by the detector and can be related to the various properties of the medium.

The typical lasers used as light sources are pulsed, which provide a higher peak power than the continuous-wave lasers. Also the short pulse time is useful for good temporal resolution. Some of the widely used laser sources are Nd:YAG laser, dye lasers, excimer lasers, and ion lasers. The light from the laser (usually a beam) is passed through a set of lenses and/or mirrors to form a sheet, which is then used to illuminate the medium. This medium is either made up of fluorescent material or can be seeded with a fluorescent substance. The signal is usually captured by a CCD or CMOS camera (sometimes intensified cameras are also used). Timing electronics is often used to synchronize pulsed light sources with intensified cameras.

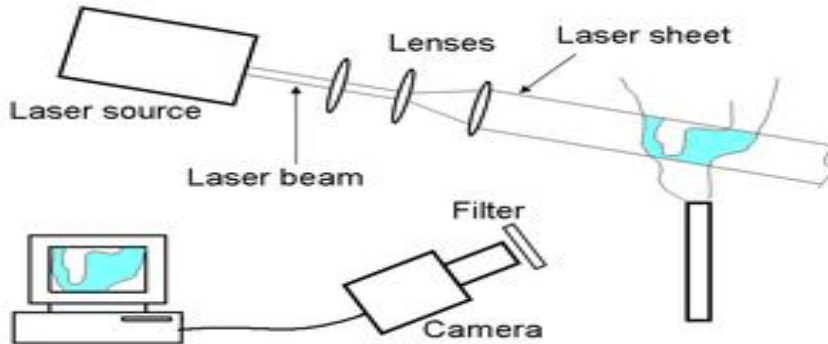


Figure (1.5) Laser induced fluorescence (LIF) setup

Laser induced fluorescence technique employs electro – optics components and can therefore gain the advantages of their peculiarities , such as in setting – up diagnostics tools, to be local and/or remote, in real time, and to operate with low radiation exposure so that the sampled object is not disturbed or damaged at all . In detail, Laser induced fluorescence (LIF) offers the advantages of being :

- Fast (the detection of a substance can be performed in a fraction of a second).
- Remote (the system and the target can be meters apart).
- Sensitive (better than parts – per - million).
- Specific substances can be recognized by their spectroscopic fingerprint.
- User – friendly (the system can be deployed in few minutes and does not require a specifically trained user) [15].

1.4.3 LIDAR Techniques

LIDAR, which is an acronym for light detection and ranging, is a measurement technique in which pulsed laser radiation is transmitted into the atmosphere and back – scattered light is detected at a certain time delay in a radar like fashion. The most common use of the lidar techniques is for ranging, where the distance to a target is measured. Laser range finders have many applications, many of which are of a military nature. However, the technique is also used in land surveillance and in a number of interesting scientific contexts [2] .

LIDAR works in a similar way except that the source of radiation is a pulsed laser and the wavelength lies in the infrared, visible or ultraviolet region. LIDAR provides a very powerful technique for investigation of the earth's atmosphere both in the troposphere, up to 14 km, and the stratosphere, in the range 18 – 50 km above the surface. It is the use of LIDAR devices as tools for spectroscopic measurements on the various gases present in the atmosphere which concerns us here. These include ozone, carbon dioxide, and all those molecules regarded as atmospheric pollutants [16]. Figure (1.6) shows a schematic diagram of LIDAR.

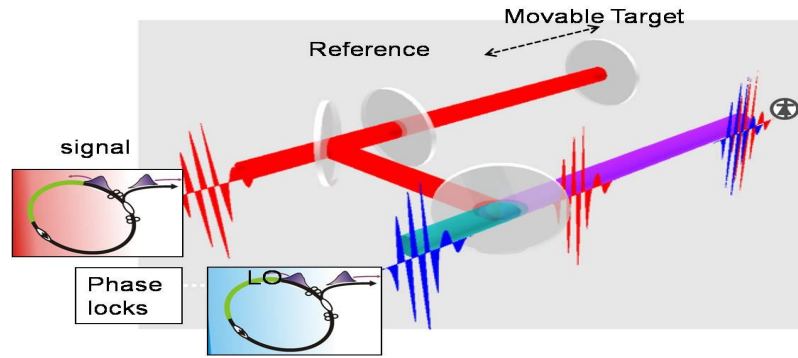


Figure (1.6) Schematic diagram of LIDAR

1.5 Laser Induced breakdown spectroscopy (LIBS).

Laser-induced breakdown spectroscopy (LIBS) is a method of atomic emission spectroscopy (AES) that uses a laser-generated plasma as the hot vaporization, atomization, and excitation source. Because the plasma is formed by focused optical radiation, the method has many advantages over conventional AES techniques that use an adjacent physical device (e.g. electrodes, coils) to form the vaporization/excitation source.

LIBS measurement is carried out by forming a laser plasma on or in the sample and then collecting and spectrally analyzing the plasma light. Qualitative and quantitative analyses are carried out by monitoring emission line positions and intensities.

Laser induced breakdown spectroscopy (LIBS) uses a laser pulse to atomize a sample. The components of the sample emit electromagnetic radiation, and the elemental composition can be determined via a spectrometer. The spectra contain qualitative and quantitative information that may be used to determine sample identity or amount of sample constituents [17]. LIBS can be a valuable tool for forensic analysis due to its minimal sample preparation, transportable capabilities and wide range of spectral sensitivity [18]. LIBS has the ability to analyze samples in the solid, liquid, gaseous or aerosol states [19].

1.5.1 The LIBS method in brief

A typical LIBS set-up is shown in Figure (1.7). Pulses from a laser are focused on the sample using a lens and the plasma light is collected using a second lens or, by a fiber optic cable. The light collected by either component is transported to a frequency dispersive or selective device and then detected.

Each firing of the laser produces a single LIBS measurement. Typically, however, the signals from many laser plasmas are added or averaged to increase accuracy and precision and to average out non-uniformities in sample composition. Depending on the application, time-resolution of the spark.

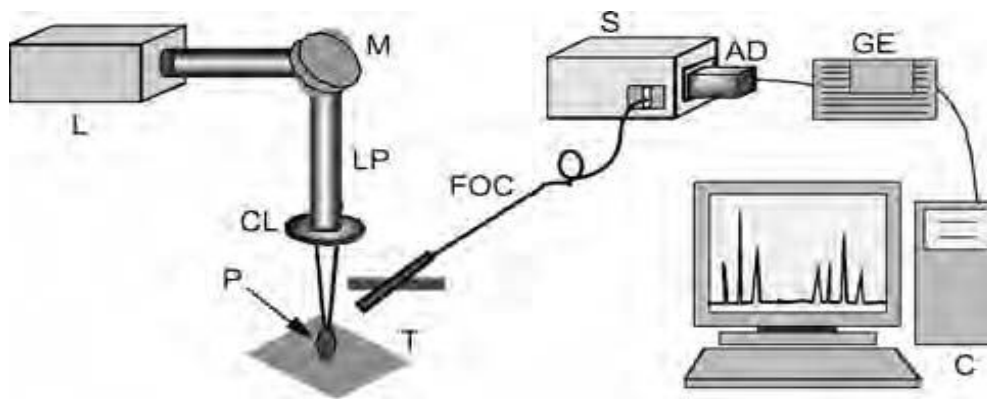


Figure (1.7) Diagram of a typical laboratory LIBS apparatus. Here: L = laser; M = mirror; LP = laser pulse; CL = lens; P = plasma; T = target; FOC = fiber optic cable; S = spectrograph; AD = array detector; GE = gating electronics; C = computer.

1.5.2 Components for a LIBS setup

The main components include a laser, a method of spectrally selecting one or many narrow regions of the spectrum to monitor emission lines, and a method of detecting the spectrally selected light. The specifications of each component of a LIBS instrument as well as the method of sampling to be used will depend on the application. Factors to consider

include: (1) the elements to be monitored (number and type), (2) the characteristics of the sample (compositional complexity, homogeneity, etc.), (3) the type of analysis (e.g. a qualitative versus quantitative measurement), and (4) the state of the sample (e.g. gas, liquid, or solid).

1.5.3 Laser systems for LIBS

Laser Parameters important in the specification of the LIBS include: (1) pulse energy, (2) pulse repetition rate, (3) beam mode quality, (4) size/weight, and (5) cooling and electrical power requirements. The wavelength of the laser beam is not an important factor in most cases but can be a consideration if factors such as eye safety, reliability, and wavelength of scattered light are critical. On the other hand, a particular wavelength may couple more efficiently into a specific material [20].

Solid-state lasers, in particular, flashlamp-pumped pulsed and Q-switched Nd:YAG lasers having pulsewidths in the range 6–15 ns, are typically used for LIBS measurements. These lasers are a reliable and convenient source of the powerful pulses needed to generate the laser plasmas. In addition, compact Nd:YAG lasers are available for use in portable instrumentation.

The fundamental wavelength of the Nd:YAG laser (1064 nm) can easily be converted to shorter wavelengths (532, 355, and 266 nm) using a crystal via passive harmonic generation techniques which may have certain advantages in terms of increased energy coupling into a particular sample. Typically, however, the 1064 nm wavelength is used because this provides the highest power density. Other types of lasers, most notably the pulsed CO₂ laser (10.6 μm wavelength) and the excimer laser (typical wavelengths of 193, 248 and 308 nm) have been used for LIBS. In comparison with solid-state lasers, however, these lasers require more maintenance (e.g. change in gases) and special optical materials because

their wavelengths lie in the far infrared and ultraviolet spectral regions, respectively. For this reason these lasers are not widely used. As noted above, the Nd:YAG laser is available commercially in a wide range of sizes. These range from laboratory-based models which can output 1 J or more of pulse energy at repetition rates between 10 and 50 Hz to small hand-held versions with a repetition rate of 1 Hz and a pulse energy of about 17 mJ. The laboratory models require 208 VAC electrical services of at least 20 A and may require external water cooling or at least a heat exchanger.

1.5.4 Detectors

The type of detector used for LIBS measurements is determined by the method of spectral selection. The simplest photodetectors include photomultiplier tubes (PMT) and photodiodes (PD). These consist of a photosensitive material that generates a signal proportional to the amount of incident light. Common examples of array detectors include photodiode arrays (PDA), charge-coupled devices (CCD) and charge-injection devices (CID). Array detectors are used with spectrographs to record the continuous spectrum presented at the focal plane of the instrument. The PDA/CCD/CID devices are light-integrating devices. That is, they collect incident light for a period of time, typically microseconds, and then the charge collected on the device is read out. This difference between the two types of detectors is based on the method of readout. Because PDA/CCD/CID are array devices, the signals stored on each pixel are read out sequentially, one pixel at a time, limiting the speed with which the entire array can be read out and readied for another measurement. LIBS measurements are typically carried out by using time-resolved detection of the plasma light. It is most important to remove the spectrally broad white light that occurs at early times (0–1 μ s)

after plasma formation. With the PDA/CCD/CID devices this is accomplished by using a microchannel plate (MCP) in front of the array detector.

1.5.5 forming the LIBS plasma in a solid

The phenomena of Breakdown on surfaces and ablation are complex. Depending on the pressure above the surface. Breakdown thresholds are two to four orders of magnitude lower than in the case of gas targets. For low pressures above the surface, higher ion stages are reached for the same incident intensities. The long wavelength is absorbed to a much greater extent in the plasma above the surface because absorption varies as the square of the wavelength (λ^2).

This effectively shields the surface from absorption of the trailing edge of the laser pulse. At short wavelengths, a higher percentage of the laser energy impacts the surface. LIBS on surfaces depend on the ablation of material into the plasma volume. In the case of LIBS, however, it is best to concentrate on optimizing the signal, not necessarily the amount of material ablated. In some cases high material content can degrade plasma properties and lead to inferior performance. When the laser energy is focused on solids in vacuum, higher stages of ionization are reached for the same intensity on target. The post-breakdown expansion differs from that in an ambient atmosphere because of the absence of collisions with the background atoms or molecules. The femtosecond pulse length arena is another where ablation studies are proceeding [21].

1.5.6 Advantages & disadvantages of LIBS

There are advantages and disadvantages of LIBS technique. First of all, LIBS technique has little or no sample preparation. This is an advantage because it eliminates possible contaminations and loss of analyte throughout the sample preparation steps. Besides, LIBS may be easily

applied to all forms of samples, solid, liquid and gas. Even analyses of very hard samples are permitted. For solid samples depth profiling and lateral resolution is possible. This advantage arises from the fact that LIBS systems use only small amounts of sample. Craters with a few micrometers of diameters are obtained with suitable optics. By the help of the use of fiber optic cables, LIBS system can be applied as a remote analysis technique. Further more, the compact portable LIBS set-ups enable field analysis. One of the major advantages of LIBS is its speed and ability to make multi-elemental analysis. By using suitable spectrograph equipped with a multi channel detector, analysis of dozens of elements in a single laser shot may take just a second.

Contrary to the advantages of LIBS, there are some disadvantages. Since the energy of laser may vary from one shot to another, the response monitored changes. This 5-10% energy variation may lead to a problem during low level of quantification. Therefore, in order to eliminate this disadvantage, several measurements may be averaged. Also, during the analysis of solids, the surface composition may be different than the bulk composition. Since the crater formed by the focused beam is just a few micrometers in size and depth, the investigated area may not be a representative of the whole sample. As a result of the above facts, the analytical figures of merit are not as good as the other widely used atomic spectroscopic techniques such as ICP-OES and AAS.

1.6 Literature Review

In 2007 Walid Tawfik Y. Mohamed from the National Institute of Laser Enhanced Science (NILES), Dept. of Environmental applications, Cairo University used in his study an accurate LIBS setup to identify different seawater samples (with different salinities) using an optical fiber probe. In doing so, he study the matrix effect on the plasma characterization of

seawater samples. The obtained results showed that both electron temperature and density are related to the matrix composition and change if the matrix changes. Moreover, Tellurium (Te) and Neon (Ne) could be measured using any of the three elements (Na, Ca, and Mg) in the seawater matrix. This means that *Te* and *Ne* represent a fingerprint plasma characterization for a given seawater sample and its salinity could be identified using only one element without need of analysis of the rest of elements in the seawater matrix. This could be done by building a database containing the determined values of *Te* and *Ne* for a wide range of seawater salinities. Then the salinity of the unknown seawater sample could be identified just by comparing its measured *Te* and *Ne* values with the previously stored values in our database. The obtained results indicate that it is possible to improve the exploitation of LIBS in the remote on-line environmental monitoring, by following up only a single element as a marker to identify the seawater matrix composition and salinity without need to analyze that matrix which saves a lot of time and efforts.

In 2010 Dilek ARICA ATEŞ from the Graduate School of Engineering and Sciences of İzmir Institute of Technology studied the laser induce breakdown spectroscopic of metal aerosols generated by pneumatic nebulization of aqueous solutions.

In that study, an aerosol generation system has been designed, constructed and coupled to a LIBS system that has been set-up from the commercially available parts. Pneumatic nebulization method has been used to generate particles and a special heating/cooling and membrane drying steps are conjuncted.

Two different experimental LIBS set-us, horizontal and telescopic, were used to form plasma. In telescopic setup, in which the laser beam has been directed from the top of the sample chamber, the plasma image is

formed vertically along the slit height of the spectrograph. This way, the variation in plasma position on the slit due to shot to shot variation of the laser pulses has been reduced. The experimental parameters such as flow rate, heating and cooling temperatures, delay times, gate widths, detector gain and laser energies have been optimized for sodium, calcium, magnesium and potassium elements.

Sodium, calcium, magnesium and potassium elements have been studied and the detection limits have been found to be 1, 0.6, 1.5 and 16.3 mg/L respectively. These values for detection limits are comparable to the values given in literature. Besides, real samples mineral water and tap water have been analyzed. Also standard addition of calcium and magnesium on sodium element has shown that the sodium analyte is not highly affected by the presence of the matrix elements.

The efficiency of the heating/cooling unit and the membrane dryer has been demonstrated. 90 % of the aqueous analyte solution has been converted into aerosol. Particle size measurements have been performed. The particles size range has been found as 4.3 μm for sodium. The membrane dryer has reduced the particle size of aerosol droplets to 0.5 μm .

In July 2012 Al Muslet, J. J. Lasema and S. Y Mohamed identified of the constituents of some Sudanese crude oil and soil using (LIBS). The emission lines of different elements were identified in the region from 230 to 950nm.

Organic compounds showed specific spectral features including sequences of the CN violet system and C_2 swan system, and H, C, N and O atomic and ionic lines. The principle for identification of organic compounds was on their spectral features and on the integrated intensity ratios of the molecular (CN, C_2) and atomic ($\text{H}\alpha$, C_2).

The main objective of this work was to demonstrate that new developments in LIBS technique are able to provide reliable qualitative and quantitative analytical evaluation of several heavy metals in soils, with special focus on the element chromium (Cr), and with reference to the concentrations measured by conventional ICP spectroscopy. The preliminary qualitative LIBS analysis of five soil samples and one sewage sludge sample has allowed the detection of a number of elements including Al, Ca, Cr, Cu, Fe, Mg, Mn, Pb, Si, Ti, V and Zn. Of these, a quantitative analysis was also possible for the elements Cr, Cu, Pb, V and Zn based on the obtained linearity of the calibration curves constructed for each heavy metal, i.e., the proportionality between the intensity of the LIBS emission peaks and the concentration of each heavy metal in the sample measured by ICP.

1.7 The aim of this work

This work aimed to investigate the spectroscopic changes and elements in five different samples of teeth with caries. The LIBS were recorded for three regions in each tooth (Health, Caries and the edge between the health and caries regions). This study is based on the use of laser induced breakdown spectroscopy (LIBS) technique in which Q-Switched Nd-YAG laser is focused on the sample which leads to plasma emission of discrete lines.

These lines are the fingerprints of the atoms and ions constitute the sample. By recording these emission lines one can identify the elements of each tooth. The results of the three region will be compared for each sample to determine the spectroscopic changes that happen due to caries.

CHAPTER TWO

The Experimental Part

2.1. Introduction:

This chapter illustrates the materials used in this work and the equipments in addition to the experimental procedure.

2.2. The experimental setup

In this study the experimental setup consist of four basic parts as shown in figure (2-1). These parts were the laser, spectrometer, optical fiber and the software. The arrangement is represented schematically in figure (2.2).



Figure (2-1) The Experimental setup

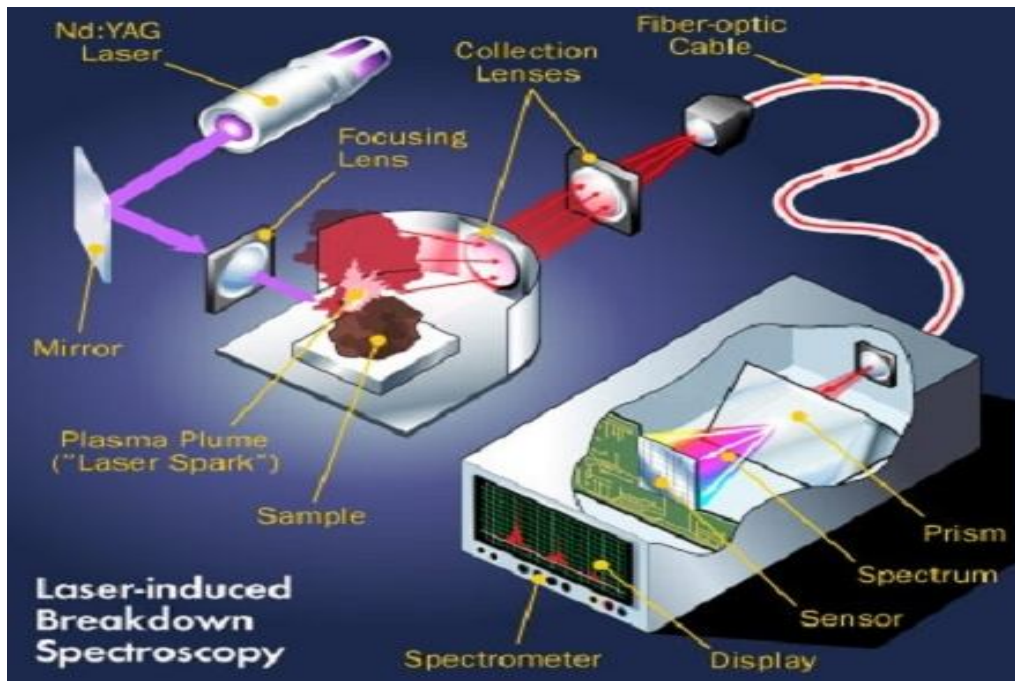


Figure (2.2) Schematic diagram of the setup

2.2.1. The Laser

The type of laser used in this work is Q-Switched Nd : YAG laser. It was used to deliver laser beam at 1064 nm. Supplied from XSD Hua Zhong precision instrument - model LRH786T with 10ns pulse duration and (1-5) Hz repetition rate.

The pulse energy of this laser was adjustable depending on the applied pumping the flashlamps voltage. The specifications of this laser are depicted in table (2-1).

Table (2.1): Specifications of the Q- switched ND:YAG Laser LRH786T:

Cooling system	Air & water cooling circulation
Dimension	38cm 36cm 28cm (L*W*H)
Model	LRH786T
Operation interface	6 dual color LCD

Pulse duration	<10ns
Pulse energy	1064nm (max 1000 mJ) & 532nm (max 500mJ)
Power	400 W
Power supply	100/110V, 50-60 HZ OR 230 260 V . 50- 60 HZ
Repetition rate	(1-5) Hz adjustable
Spot size	(2 – 5) mm
Wavelength	1064nm, 532nm
Working period	Continuously working for 1- 2hours

The population density of the upper laser level ions is usually clamped at relatively low value due to the electronic energy levels of the Nd ions in the laser rod. If the pumping flashlamp that fired to produce broadband light is sufficiently intense, a population inversion is established and a photon passing through the laser rod at the same frequency as the lasing transition will experience gain or amplification by including decay of some of the ions from the upper to the lower state.

The laser rod is surrounded by resonant cavity composed of two mirrors in which some of this amplified light is directed back into the rod, significant amplification can be achieved. The high power needed to form microplasma for LIBS can be easily achieved using (10 ns) pulse duration.

2.2.2. The Spectrometer

The spectrometer used in this work is type USB4000 supplied from ocean features a 16-bit A/D, 4 total triggering options, a dark-level correction during temperature changes, and a 22-pin connector with 8 user-programmable GPIOs. As shown in figure (2-3).

The USB4000 is responsive from 200-1100 nm, but the specific range and resolution depends on the grating and entrance slit selections.

The USB4000 is perfect for applications where enhanced electronics, high resolution and fast integration times are required.

Data programmed into a memory chip on each USB4000 includes wavelength calibration coefficients, linearity coefficients, and the serial number unique to each spectrometer.



Figure (2.3) spectrometer USB4000

The USB4000 Spectrometer may be connected to a computer via the USB port or serial port. When connected through a USB 2.0 or 1.1, the spectrometer draws power from the host computer, eliminating the need for an external power supply. The USB4000, like all USB devices, can be controlled by SpectraSuite software, a completely modular, Java-based spectroscopy software platform that operates on Windows, Macintosh and Linux operating systems. Figure (2-4) shows how light directed through the asymmetrical crossed Czerny-Turner optical bench, which has no moving parts that can wear or break.

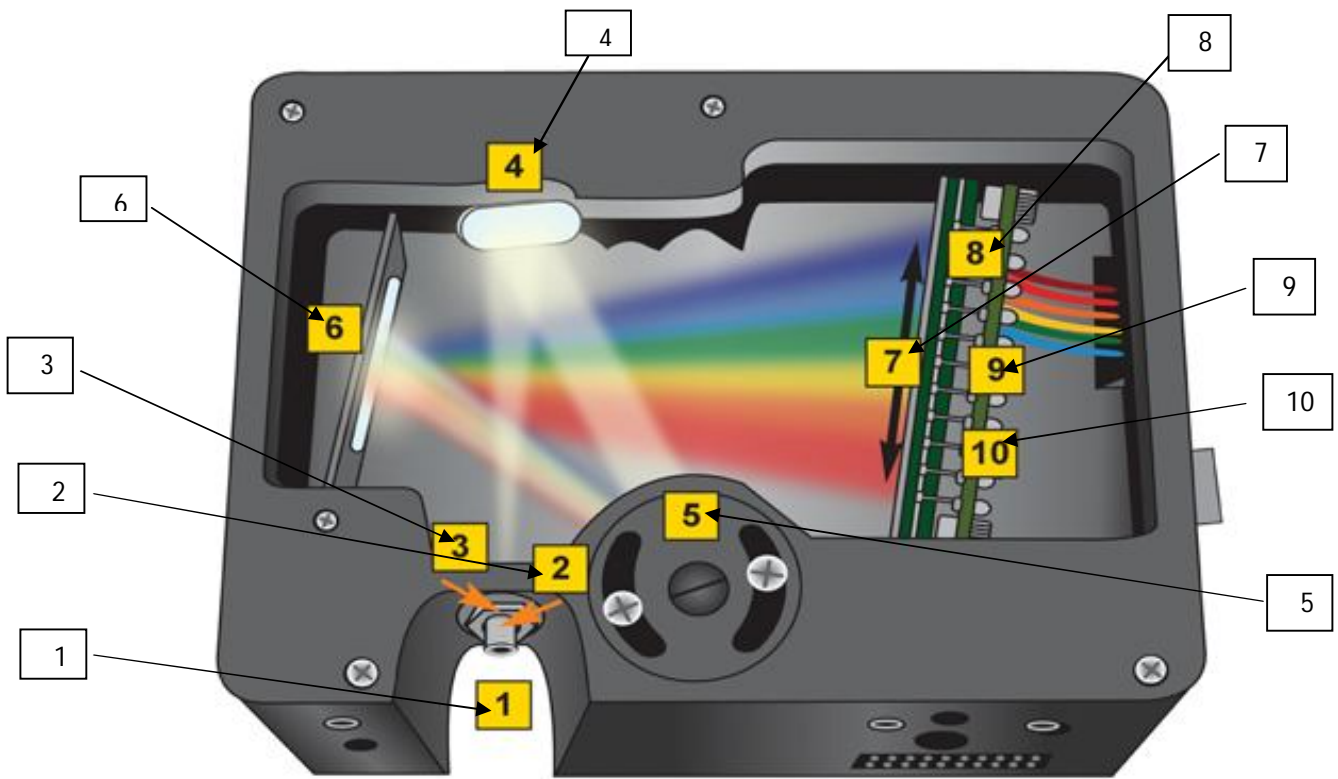


Figure (2.4) the propagation direction of light inside the spectrometer
USB4000

1. **SMA 905 connector** : Light from a fiber enters the optical bench through the SMA 905 connector. The SMA 905 bulkhead provides a precise locus for the end of the optical fiber, fixed slit, absorbance filter and fiber clad mode aperture.
2. **Fixed Entrance Slite** : Light passes through the installed slit, which acts as the entrance aperture. The slit is fixed in the SMA 905 bulkhead to sit against the end of a fiber.
3. **Longpass Absorbing Filter** : Is installed between the slit and the clad mode aperture in the SMA 905 bulkhead. The filter is used to block second- and third-order effects or to balance color.
4. **Collimating Mirror** : The collimating mirror is matched to the 0.22 numerical aperture of our optical fiber. Light reflects from this

mirror, as a collimated beam, toward the grating. One can install a UV absorbing SAG+ mirror or a standard mirror.

- 5. Grating & Wavelength Range :** Install the grating on a platform that rotate to select the starting wavelength that have specified. The grating permanently fixed in place to eliminate mechanical shifts or drift.
- 6. Focusing Mirror :** This mirror focuses first-order spectra on the detector plane. Both the collimating and focusing mirrors are made in-house to guarantee the highest reflectance and the lowest stray light possible.
- 7. L4 Detector Collection Lens :** This cylindrical lens, made in-house to ensure aberration-free performance, is fixed to the detector to focus the light from the tall slit onto the shorter detector elements. It increases light-collection efficiency.
- 8. Detector :** There are 3648-element Toshiba TCD1304AP linear CCD array detector for the USB4000. Each pixel responds to the wavelength of light that strikes it. Electronics bring the complete spectrum to the software.
- 9. OFLV Variable Long pass Order – sorting Filter:** The proprietary filters precisely block second- and third-order light from reaching specific detector elements.
- 10. UV4 Detector Upgrade :** The detector's standard BK7 window is replaced with a quartz window to enhance the performance of the spectrometer for applications <340 nm.

2.2.3. Optical Fiber

Optical fiber is One of the most important element's in the set up of work it used to collect spectra was supplied by ocean optics . The main component for optical fiber are core, cladding and buffer coat

(primary protective coating) . It is type UV – VIS model QP600-2-UV-BX 600 mm diameter and two meter length silica core . The core is surrounding by doped-fluorine silica cladding then the a buffer material is applied.

Precision SMA 905 Connectors terminate the assembly and are precisely aligned to the spectrometer's slit to ensure concentricity of the fiber. Finally, captive end caps protect the fiber tips against scratches and contaminants .

2.2.4. The Software

In this work a software type SpectraSuite was used as a spectroscopy software platform that operates on Windows, Mac OS and Linux operating systems. The software can control virtually any Ocean Optics USB spectrometer and device with ease.

SpectraSuite easily manages multiple USB spectrometers – each with different acquisition parameters – in multiple windows, and provides graphical and numeric representation of spectra from each spectrometer. SpectraSuite provides the user with advanced control of episodic data capture attributes. For instance, a user can acquire data for a fixed number of scans or for a specific interval. Initiation of each scan can be externally triggered or event-driven. Captured data is quickly stored into system memory at speeds as fast as 1 scan per millisecond, with speeds limited by hardware performance.

2.3 The materials

The materials used were five teeth with caries. The samples were collected from the hospital of medical arms. Formalin was used to save the samples.

The structure of the human tooth is shown in figure (2.6). It is made of approximately 95% (by weight) hydroxyapatite, 4% water, and 1% organic matter. Hydroxyapatite is a mineralized compound with the chemical formula $\text{Ca}_{10}(\text{PO}_4)(\text{OH})_2$. Its substructure consists of tiny crystallites which form so-called enamel prisms with diameters ranging from 4 μm to 6 μm . The crystal lattice itself is intruded by several impurities, especially Cl^- , F^- , Na^+ , K^+ , and Mg^{2+} .

The dentin, on the other hand, is much softer. Only 70% of its volume consists of hydroxyapatite, whereas 20% is organic matter – mainly collagen fibers – and 10% is water. The internal structure of dentin is characterized by small tubuli which measure up to a few millimeters in length, and between 100nm and 3 μm in diameter. These tubuli are essential for the growth of the tooth. The pulp, finally, is not mineralized at all. It contains the supplying blood vessels, nerve fibers, and different types of cells, particularly odontoblasts and fibroblasts. Odontoblasts are in charge of producing the dentin, whereas fibroblasts contribute to both stability and regulation mechanisms. The pulp is connected to peripheral blood vessels by a small channel called the root channel . The tooth itself is embedded into soft tissue called the gingival which keeps the tooth in place and prevents bacteria from attacking the root [22].

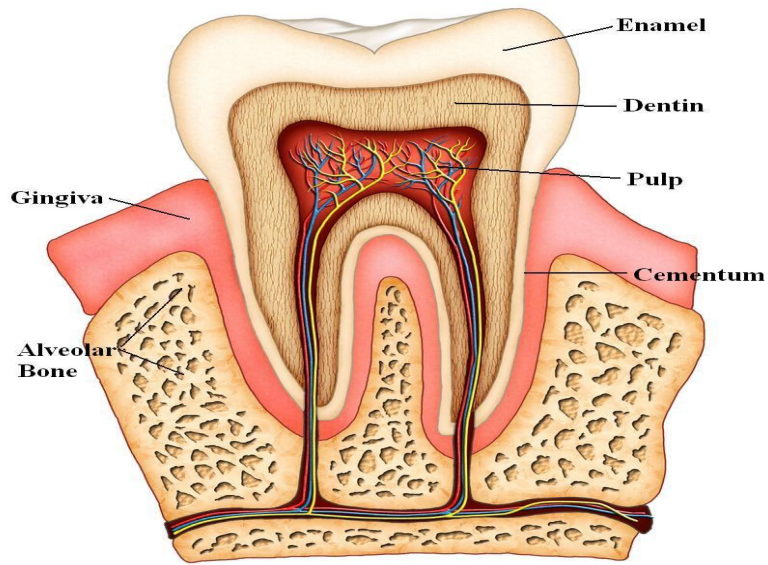


Figure (2.5) Human tooth and all of its magical layers.

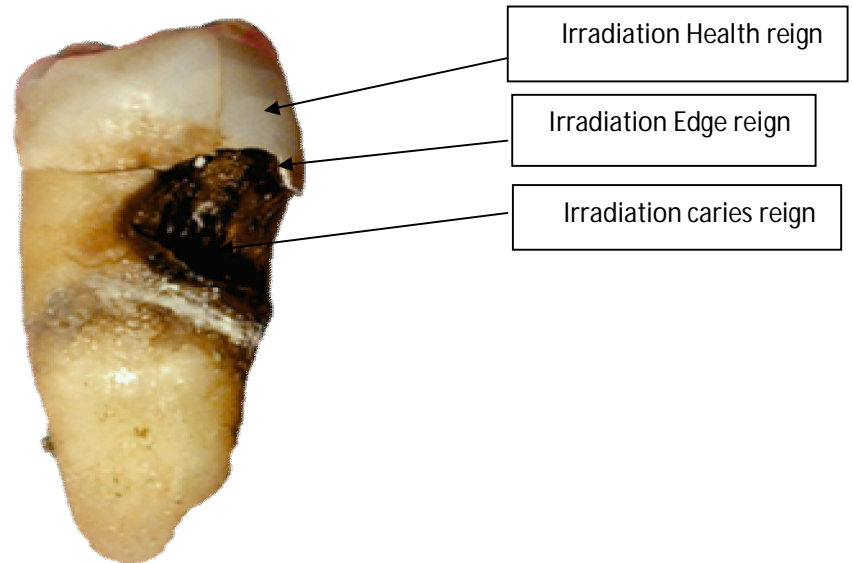


Figure (2.6) The irradiation of the three regions (health, edge and caries) in human tooth

2.4. The Experimental Procedure

The experimental procedure was done as follows:

1. The setup was arranged as shown in figure (2.1)
2. The laser energy was adjusted by the flash lamp voltage in order to obtain sufficient peak power needed to form plasma.
3. Then the spectrometer was connected to the PC through USB cable and the program spectrasuit was launched.
4. The desired parameters (integration time, scan to average) were set to ensure accurate data.
5. A laser pulse was fired in the air without the sample and the emission spectrum was recorded and saved as dark spectrum that would be subtracted when getting the sample spectrum. This procedure is important because flash lamp of the laser emit radiation contain UV/VIS with intensity often higher than the signal of the sample under testing .
6. Before starting the sample acquisition, the optical fiber terminal was aligned during laser firing till maximum intensity was collected and appeared on the screen. This was done to enhance signal to noise ratio.
7. After that the sample was put and a pulse from the laser was fired and the emitted spectrum was recorded. This process was repeated three time for each sample in three regions (Health, caries and edge between health and caries region).
Figure (2.6) Show the irradiation of the three regions (health, edge and caries) in human tooth.
8. The LIBS spectrum of the sample was processed by subtracting the dark spectrum.

9. By referring to the atomic spectra database, the atoms and ions of the LIBS were identified .
10. The same above procedure was done for the other samples three times for each sample.
11. A comparison was done between each sample for the three cases (Health, caries and edge) then a comparison was done between all samples.

CHAPTER THREE

Results and Discussion

3.1 Introduction

In this chapter the results obtained during this work and its analyses are presented, beside the comparison between the spectra for the five teeth samples.

3.2 LIBS results

Emission spectra, in the range from 180 nm to 883 nm of the five teeth samples are shown in figures (3-1) to (3-5), respectively. The laser energy per pulse was 23.4 mJ and the pulse duration was 10 ns that lead to peak power equals 2.34×10^6 W. The power density was 1.32×10^6 W/cm². Atomic spectra database was used for the spectral analysis of the tested samples.

3.2.1 Tooth No. 1:

Figures (3-1a), (3-1b) and (3-1c) show the LIBS spectra of teeth no.1 (the healthy , edge and caries regions respectively).

Table (3-1) list the analysis of these spectra and the comparison between them.

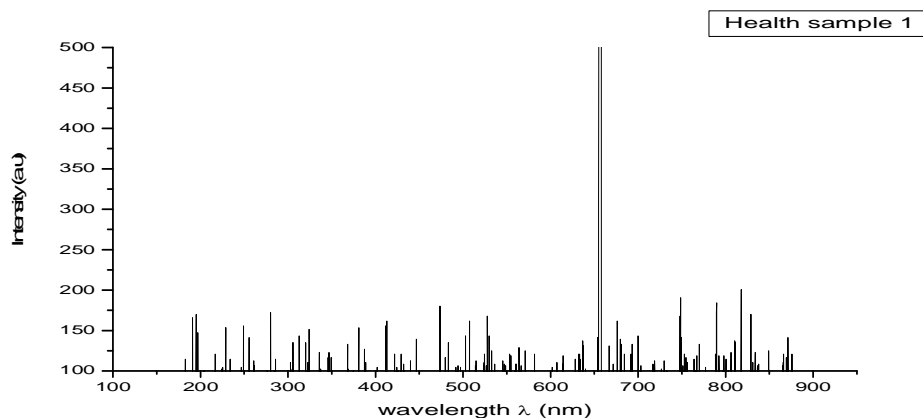


Fig.(3.1a) LIBS emission spectrum of tooth No 1 (health region)

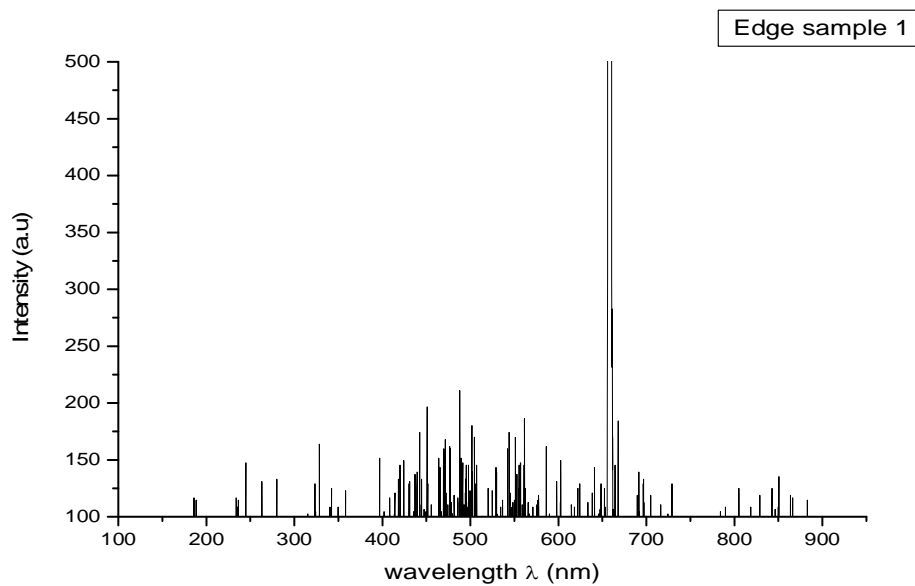


Fig.(3.1b) LIBS emission spectrum of tooth No. 1 (edge region)

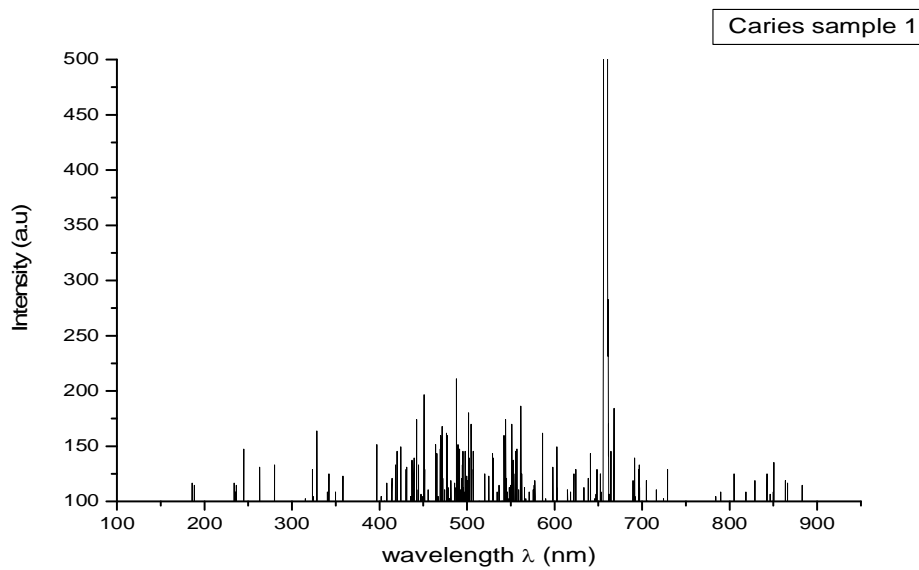


Fig.(3.1c) LIBS emission spectrum of tooth No. 1 (caries region)

Table (3.1): analysis of LIBS emission spectrum for tooth No 1 (health, edge and caries)

Recorded wavelength λ (nm)	Health	Edge	Caries	Elements and ions
	Intensity (a.u)	Intensity (a.u)	Intensity (a.u)	
183.472	123.6	0	0	Mo VII
185.254	0	0	125.17	Co II
187.735	0	153.03	0	W III
188.804	0	0	123.6	Ru II
191.640	172.81	0	0	Ba III
194.844	174.83	0	0	Ag III
197.331	153.03	0	0	W II
209.760	0	154.38	0	B III
214.383	0	158.2	0	Rb II
216.867	125.84	0	0	Fe II
225.030	110.56	0	0	Fe II
227.167	0	133.93	0	Co II
229.651	158.88	0	0	Pd II
233.916	0	0	122.92	W II
236.404	0	0	121.57	Fe II
242.080	0	127.42	0	Rb III
247.051	111.24	0	0	Eu III
247.769	0	144.27	0	N IV
249.195	160.9	0	0	Fe II
250.251	0	119.33	0	Fe II
256.290	148.54	0	0	Be II
260.910	118.65	0	0	W II
262.687	0	0	136.18	Fe II
266.230	0	154.38	0	Fe I
270.855	0	125.17	0	Ba III
280.091	0	0	138.43	Fe II
280.443	178.65	0	0	Hg I
282.574	0	135.51	0	Fe II
286.130	118.65	0	0	Ti II
297.490	0	152.36	0	Xe III
302.471	114.83	0	0	Fe II
304.600	0	121.57	0	Sc I
306.024	143.37	0	0	Rb I
306.730	0	121.57	0	Xe II
312.773	147.87	0	0	W II

314.900	0	0	111.24	Xe II
315.967	0	121.57	0	Ho II
320.940	142.7	0	0	Xe IV
323.072	0	0	132.58	Mn I
324.493	155.96	0	0	Sc II
329.822	0	0	167.64	Mn I
333.370	0	119.33	0	W I
335.853	128.78	0	0	Fe II
337.991	0	111.24	0	Ti II
340.470	0	0	114.83	W I
342.604	0	111.24	130.34	Yb I
347.581	128.76	0	0	Na II
349.710	121.57	0	114.83	Fe I
352.903	0	113.48	0	Co I
356.455	0	125.17	0	Fe I
357.522	0	0	128.09	W I
358.591	0	137.75	0	W I
365.690	0	113.48	0	Os I
368.194	139.78	0	0	Ne II
380.975	160.9	0	0	Sm II
382.040	0	131.91	0	Hg I
387.718	0	158.2	0	Pr II
388.071	132.36	0	0	Tc I
392.338	0	119.33	0	Dy II
396.950	0	0	157.98	Fe III
398.029	0	152.36	0	W I
401.560	0	133.93	111.91	Fe I
401.922	111.91	0	0	W I
408.677	0	0	122.92	Ne II
411.167	166.07	0	0	W I
413.091	168.99	0	0	Na I
414.349	0	150.11	0	Fe I
414.351	0	0	125.84	Tb I
417.926	0	0	139.1	Cr I
418.973	0	149.44	0	Al III
420.041	0	0	153.03	W I
421.469	126.52	0	0	Xe II
424.659	0	111.24	156.63	F II
425.011	113.48	0	0	Fe I
429.635	126.52	0	0	Mg III
430.332	0	0	138.43	W II

430.352	0	117.3	0	W I
431.765	116.4	0	0	W I
434.960	0	0	112.81	Rn I
436.375	0	142.02	0	W I
437.446	0	0	144.94	Sc II
438.505	0	154.38	0	Ar II
439.576	0	0	147.19	Fe III
439.931	119.33	0	0	W I
442.061	0	0	182.25	Au II
444.199	0	0	141.35	Mn II
447.031	146.29	0	0	Zr I
451.325	0	0	202.02	W I
454.853	0	135.51	0	Be I
455.910	0	0	117.08	W I
456.987	0	133.93	0	Ac III
461.609	0	150.11	0	Ne II
468.711	0	185.17	0	W I
471.901	0	178.65	0	Tc I
473.677	185.17	0	0	Fe I
474.382	0	228.31	117.08	Sc I
476.536	0	135.51	0	Sb II
479.364	122.25	0	0	N II
481.475	0	0	125.17	Na II
483.976	142.02	0	0	Fe I
486.120	0	0	125.17	Cr I
488.246	0	154.38	217.3	Ce II
490.373	0	150.11	0	Ti I
491.784	0	0	155.06	W I
492.148	111.24	0	0	Xe II
492.833	0	182.92	0	Ti I
494.259	111.91	0	0	Fe I
494.977	0	195.51	0	La I
495.352	0	0	152.13	Eu I
497.476	0	0	152.13	Ne I
497.854	111.91	0	0	Na I
499.950	0	0	131.69	Ti I
502.096	0	0	187.42	Am II
502.452	151.46	0	0	Ti III
504.580	0	0	175.73	Hg I
506.714	0	0	153.71	Fe I
507.053	164.72	0	0	Xe III

507.769	0	127.42	0	Sr I
510.269	0	133.93	0	Hg I
512.362	0	118.65	0	W I
515.230	118.65	0	0	Pr II
519.492	0	114.16	0	Xe II
520.564	0	0	130.34	Ge II
524.466	126.52	0	0	C III
525.173	0	0	129.66	Pr II
525.181	0	131.91	0	Co II
528.021	173.48	0	0	Al II
528.720	0	0	149.21	Ne VI
530.158	150.11	0	0	Dy I
532.204	0	115.73	0	Fe I
532.657	131.69	0	0	W I
534.410	0	0	114.83	Fe II
535.832	116.4	0	0	W I
536.922	0	0	120.67	Cs II
542.567	0	154.38	0	Th II
543.659	0	0	177.75	Fe I
545.074	120.67	0	0	P II
548.286	0	207.19	0	W I
550.755	0	132.58	173.48	Sr III
553.230	124.5	0	0	Zr I
554.302	0	0	145.62	Fe I
556.420	0	172.13	152.13	Th II
559.980	0	135.51	0	Eu I
560.352	116.4	0	0	Nb I
561.060	0	0	193.26	Ag II
563.542	136.18	0	0	Nb I
565.665	0	0	120.67	Ne I
570.291	0	0	114.83	Dy I
570.648	131.01	0	0	Nb I
571.349	0	182.25	0	Lu II
577.394	0	112.13	124.49	Th I
582.011	127.42	0	0	Kr I
587.659	0	160.45	0	Mo I
597.973	0	0	136.85	Pm I
601.558	0	133.26	0	Eu I
601.890	111.91	0	0	Fe II
602.616	0	0	153.03	Sc I
603.658	0	152.36	0	Ba III

607.574	117.08	0	0	pb II
608.321	0	140.67	0	Xe II
614.336	0	0	116.4	Ce II
614.684	123.6	0	0	Hg II
617.536	0	131.91	0	Ni I
617.891	0	0	114.16	V I
622.520	0	0	131.69	Ru I
624.631	0	0	133.93	Fe I
628.547	122.25	0	0	B II
633.168	126.52	0	0	Tb II
633.887	0	141.35	119.33	Fe I
636.362	145.62	144.27	0	Pr II
638.489	0	0	126.52	S II
640.974	0	0	148.54	Ne I
642.030	0	160.45	0	SC II
646.661	0	162.47	0	Co II
647.764	0	0	133.93	Cs II
648.776	0	147.87	0	Xe I
652.345	0	0	130.34	Pt I
659.414	0	116.4	0	Dy II
662.651	0	224.72	0	W I
664.080	0	0	152.13	Ne I
666.555	13978	0	0	Xe III
667.268	0	0	1s89.44	Fe I
670.106	113.48	0	0	Eu I
675.762	168.31	0	0	Dy I
679.353	145.62	0	0	Kr III
683.958	126.07	0	0	V I
689.271	0	0	124.49	Pr I
690.352	0	117.98	0	Pr III
691.793	0	0	145.62	Al II
693.200	139.1	0	0	Fe II
696.376	0	0	137.52	Ti I
697.450	0	109.89	0	V I
699.549	0	142.69	0	Ta I
699.966	150.11	0	0	Ga II
703.490	113.48	0	0	Si I
704.570	0	0	122.92	Hg I
709.186	0	172.81	0	Hg I
715.943	0	0	117.08	Nb I

3.2.2 Tooth No. 2:

Figures (3-2a), (3-2b) and (3-2c) show the LIBS spectra of teeth No.2 (the healthy , edge and caries regions respectively).

Table (3-2) list the analysis of these spectra and the comparison between them.

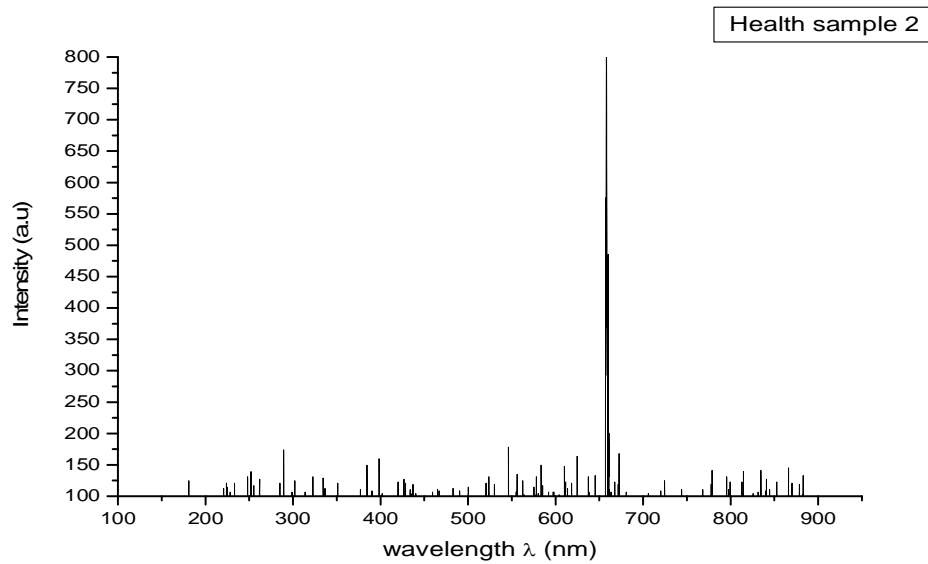


Fig. (3.2a) LIBS emission spectrum of tooth No. 2 (health region)

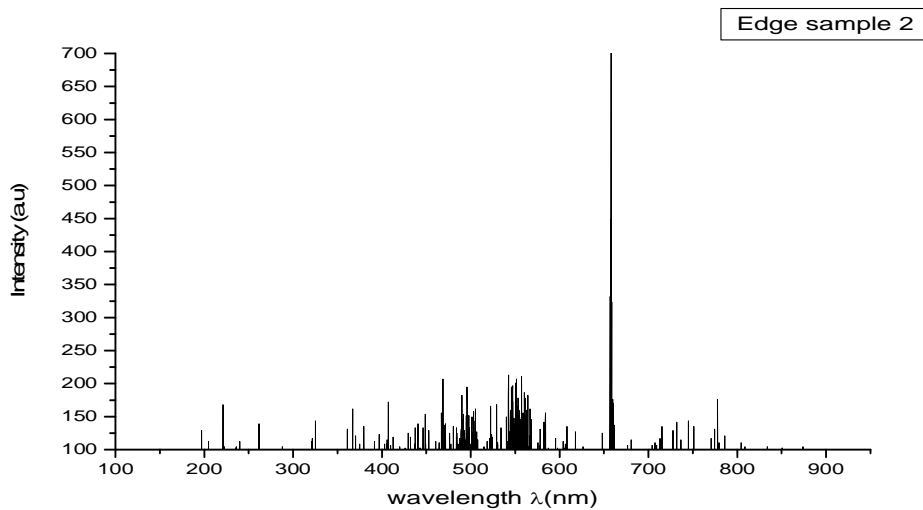


Fig. (3.2b) LIBS emission spectrum of tooth No. 2 (edge region)

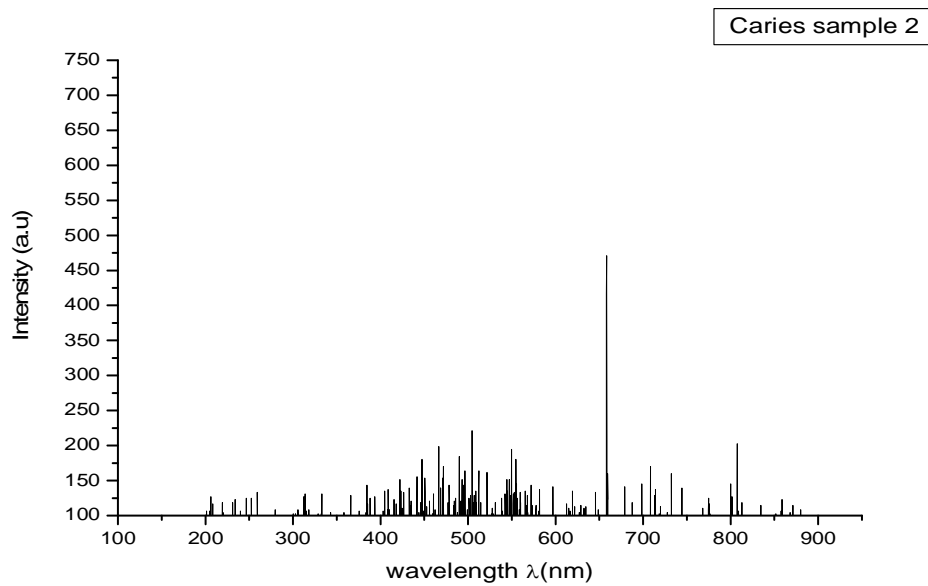


Fig. (3.2c) LIBS emission spectrum of tooth No. 2 (caries region)

Table (3.2): analysis of LIBS emission spectrum for tooth No 2 (health, edge and caries).

Recorded wavelength λ (nm)	Health	Edge	Caries	Elements and ions
	Intensity (a.u)	Intensity (a.u)	Intensity (a.u)	
193.400	133.82	0	0	V III
197.697	0	148.2	0	Co I
200.171	138.93	0	0	W II
204.430	0	133.37	0	W II
206.555	0	0	149.66	Xe II
220.066	143.65	0	143.09	Sr I
222.197	0	190	0	W III
233.200	0	0	140.53	W III
235.332	165.67	128.98	0	W II
239.950	0	133.37	129.21	Fe II
246.703	0	0	140.53	Fe II
248.832	131.46	0	0	Fe II
253.098	0	0	143.09	Fe II
255.224	156.24	0	0	W II
259.841	148.76	0	154.41	W I
261.970	0	160.67	0	Xe IV

279.735	0	0	131.4	Hg II
288.611	175.51	126.97	0	Mn II
312.773	0	0	149.66	W II
326.263	141.29	162.7	0	Mo I
333.015	133.82	0	149.67	Rb III
339.417	173.15	0	0	Tc I
344.020	0	0	131.4	Ru I
348.290	148.76	0	0	Mn II
357.182	0	0	129.21	Pa I
359.302	138.93	0	0	Ru I
361.781	0	152.25	0	Cs II
366.051	0	0	152.22	Sc VIII
370.312	146.4	145.84	0	Tb I
374.930	0	131.35	0	Be II
379.187	0	154.27	0	Dy II
383.807	138.93	0	0	Ru I
383.810	0	0	165.73	He I
390.565	182.98	0	0	Gd I
392.694	0	133.37	149.67	Zr III
394.827	202.64	0	0	Fe I
396.949	0	145.84	0	Fe III
399.088	158.6	0	0	Yb I
403.685	0	0	156.6	Sc I
407.969	0	190	152.22	Ti I
412.588	139.78	136.57	0	Fe I
419.328	0	128.99	0	Ce II
421.469	0	0	172.67	Xe II
425.728	163.31	0	0	Sc I
430.352	0	150.22	0	W I
432.479	0	0	158.79	O II
436.730	0	154.27	0	Tb II
441.356	0	164.72	0	Ne I
445.618	156.24	0	0	Co II
448.106	0	177.53	204.44	Gd II
456.621	175.51	0	140.53	Sm II
461.236	141.29	0	154.41	Sc IV
463.375	0	135.39	0	Fe I
465.505	0	0	220.51	Pm I
467.970	0	223.71	0	Ti I
472.252	0	0	190.93	Bi I
476.877	156.24	148.2	0	Ce II

479	0	0	163.54	Na VI
490.012	0	200.45	206.63	Y II
494.259	141.29	0	0	Fe I
496.768	0	211.24	186.18	W I
501.021	141.29	0	0	Ti II
505.646	0	0	240.96	La I
509.905	143.65	0	0	Ne I
512.040	0	0	181.8	Y III
514.516	0	128.99	0	C II
520.912	0	0	179.24	W I
523.050	0	185.96	0	Ar II
527.652	0	0	136.15	Cu II
529.800	0	187.98	0	Ar II
531.949	0	0	138.34	Nb I
538.688	0	0	145.28	P II
540.813	170.79	0	0	W I
543.294	0	236.18	0	Ar II
545.427	168.43	0	0	Er II
549.694	0	0	217.95	I II
556.420	0	236.18	0	Th II
560.701	141.29	0	0	Ge I
569.582	153.48	0	0	Fe II
572.061	0	0	177.05	Y I
578.466	0	156.29	0	Er I
580.598	0	0	158.79	Cu II
585.215	0	173.15	0	Rb II
596.222	0	137.42	163.54	Ce III
602.975	156.24	0	0	Nb I
604.036	0	124.61	0	Mn II
606.535	0	120.22	0	Ti II
607.243	133.82	0	0	Ti II
608.654	0	146.52	0	N II
617.891	0	136.74	0	V I
618.242	0	0	156.6	Xe I
620.760	146.4	0	0	Eu I
622.894	0	0	138.34	Ce I
626.052	0	117.19	0	Sc I
644.879	0	0	160.98	Kr I
648.019	0	135.73	0	W I
649.498	136.57	0	0	Fe I
671.538	158.6	0	0	Fe I

675.762	138.93	0	0	Dy I
676.870	0	117.19	0	Yb I
678.278	0	0	163.54	W I
680.400	0	127.98	0	Fe I
687.156	0	0	140.53	V I
693.530	143.65	0	0	Kr I
698.188	0	0	170.11	W I
704.570	0	119.21	0	Hg I
707.044	0	123.6	0	W I
709.186	0	0	193.11	Hg I
711.304	151.12	0	0	Na I
712.725	0	126.97	0	N IV

3.2.3 Tooth No. 3:

Figures (3-3a), (3-3b) and (3-3c) show the LIBS spectra of teeth No.3 (the healthy , edge and caries regions respectively).

Table (3-3) list the analysis of these spectra and the comparison between them.

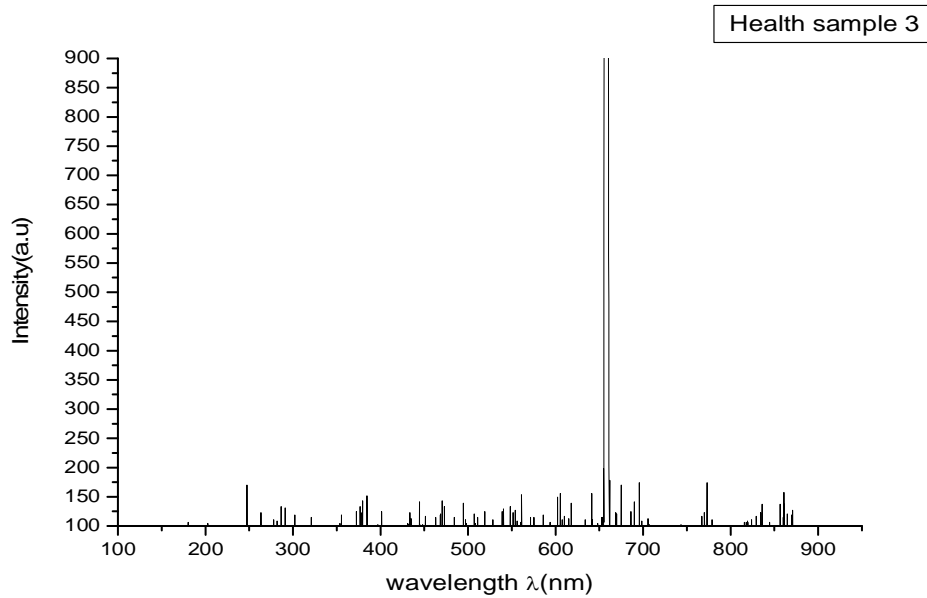


Fig. (3.3a) LIBS emission spectrum of tooth No. 3 (health region)

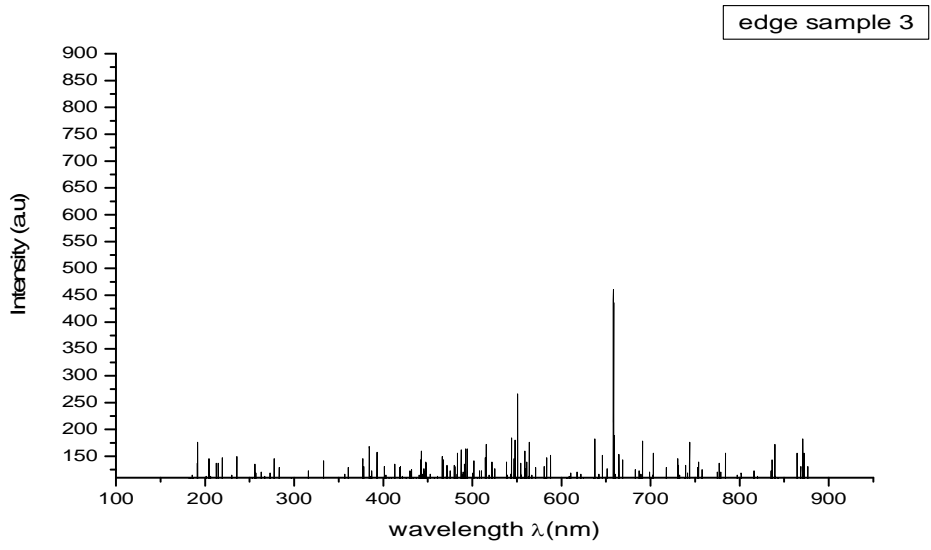


Fig. (3.3b) LIBS emission spectrum of tooth No. 3 (edge region)

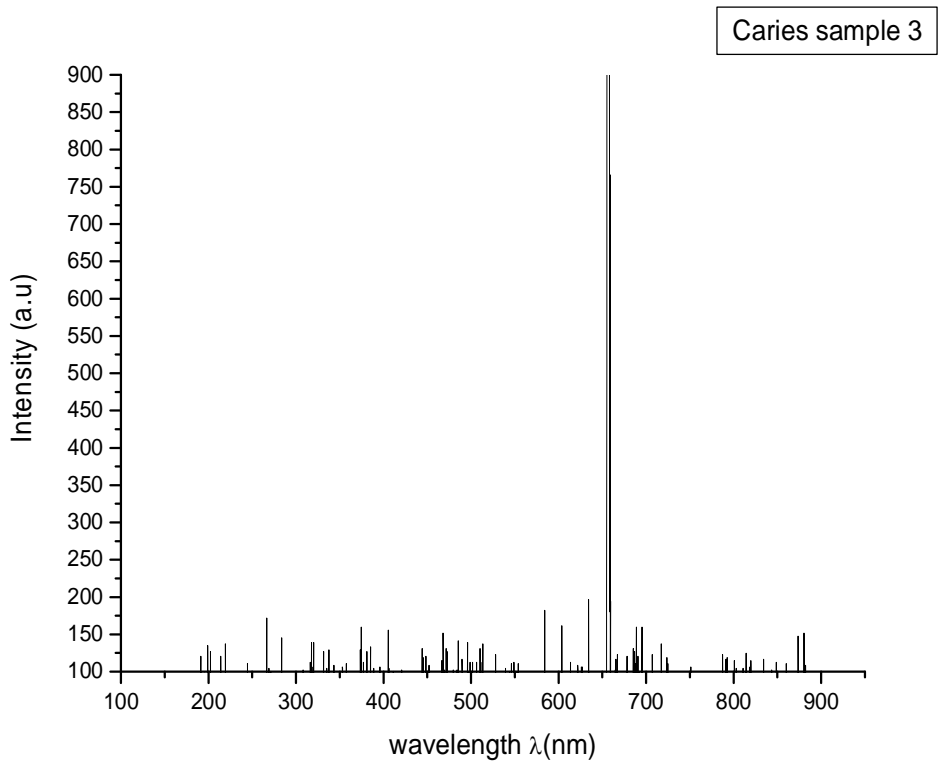


Fig. (3.3c) LIBS emission spectrum of tooth No. 3 (caries region)

Table (3.3): analysis of LIBS emission spectrum for tooth No 3 (health, edge and caries)

Recorded wavelength λ (nm)	Health	Edge	Caries	Elements and ions
	Intensity (a.u)	Intensity (a.u)	Intensity (a.u)	
180.276	133.258	0	0	Fe II
184.538	0	137.516	0	Ge II
191.286	0	187.224	144.494	Cl III
200.157	0	0	155.73	S II
202.297	135.955	0	0	Kr II
204.43	0	159.264	0	W II
213.306	0	0	141.797	W III
215.442	0	153.938	0	In III
220.058	0	159.264	138.651	Hg I
235.332	0	162.37	0	W II
244.213	0	0	133.258	Fe II
246.698	189.438	0	0	Fe II
255.224	0	148.168	0	W II
261.971	0	137.516	0	W I
264.102	147.191	0	0	Fe I
266.577	0	117.988	0	W I
266.585	0	0	186.292	W I
277.603	159.264	141.797	0	Pr II
281.854	135.955	0	0	Ca III
283.991	0	0	164.269	W II
283.997	0	145.505	0	Fe I
286.480	155.73	0	0	Mn II
290.744	158.426	0	0	Gd II
301.756	144.494	0	0	Yb II
310.634	0	0	130.561	Mo I
315.252	0	137.516	0	Sm II
317.378	0	0	144.494	Ho II
321.629	144.494	0	0	W II
330.525	0	0	141.797	Yb I
333.011	0	162.37	0	N III
337.272	0	0	144.494	Tb II
344.020	0	0	133.258	Ru I
352.903	0	0	135.955	Co I
355.036	144.494	0	0	Si III
372.797	155.73	0	0	Mn I

374.930	0	0	166.966	Be II
377.058	0	159.264	0	Si III
379.187	172.359	0	0	Dy II
381.675	0	0	141.797	Mn I
383.807	180.898	184.117	0	Ru I
385.937	0	0	144.494	Sc II
392.685	0	170.359	0	Ba III
394.816	0	0	133.258	Xe I
396.949	135.955	0	0	Fe III
401.560	151.275	147.191	0	Fe I
405.822	0	0	169.662	Gd I
412.574	0	148.168	0	Ti I
419.328	0	142.842	0	Ce II
421.444	0	0	127.865	Ru I
432.462	149.887	142.842	0	Ne II
443.481	166.966	178.792	147.191	Eu II
448.086	0	156.601	0	Xe II
463.375	162.37	144.494	0	Fe I
467.983	0	0	175.056	N III
470.128	169.662	0	0	Sc I
472.252	0	145.505	147.191	Bi I
479	0	0	130.561	Na VI
483.27	130.561	167.696	0	Kr II
485.383	0	0	153.033	W I
487.873	0	173.466	0	TH I
490.012	0	0	135.955	Y II
494.259	178.792	158.426	0	Fe I
496.768	0	0	149.887	W I
501.025	0	156.601	0	W II
505.646	0	0	122.022	La I
507.769	153.033	131.747	0	Sr I
509.905	0	0	147.191	Ne I
514.516	0	0	149.887	C II
516.655	0	187.224	0	Fe II
518.782	149.887	0	0	Ni I
520.912	0	153.938	0	W I
525.532	0	142.842	0	Mn I
527.674	138.651	0	135.955	Mo VI
538.665	0	153.938	130.561	Zr I
540.813	147.191	0	0	W I
545.427	0	0	127.865	Er II

547.549	155.73	0	0	Kr III
549.683	0	275.544	127.865	Dy I
554.302	155.73	151.275	130.561	Fe I
558.556	0	176.129	0	Cs II
560.673	169.662	0	0	Ru I
563.194	0	181.455	0	W I
567.447	0	131.747	0	Mo I
572.061	141.797	142.842	0	Y I
576.340	138.651	0	0	W I
583.078	0	156.601	0	Br II
585.208	141.797	0	194.831	Br I
587.321	0	165.033	0	Fe I
594.086	133.258	0	0	Ce I
602.975	0	0	175.056	Nb I
605.088	183.595	0	0	Pr I
609.364	144.494	137.516	0	Fe I
613.986	141.797	0	133.258	Fe I
618.242	161.123	137.516	0	Xe I
622.850	0	0	135.955	K VI
622.894	0	134.41	0	Ce I
638.122	0	195.213	0	Ti I
640.619	178.202	0	0	Te I
644.879	0	165.033	0	Kr I
647.016	135.955	0	0	Cu II
651.613	0	145.505	0	Sc III
664.768	0	167.696	0	Fe II
669.384	0	153.938	0	Ba I
669.386	147.191	0	0	Eu I
675.784	183.595	0	0	W I
678.278	0	0	138.651	W I
682.544	0	142.842	0	Er I
689.271	155.73	0	172.359	Pr I
691.401	0	198.32	0	Mo I
695.684	189.438	0	164.269	W I
698.188	0	131.747	0	W I
702.415	0	165.033	0	Re I
704.557	130.561	0	0	Hg I
707.044	0	0	141.797	W I
718.047	0	148.168	149.887	Kr I
724.441	0	0	138.651	Yb I
731.171	0	156.601	0	Ar I

740.050	0	151.275	0	Xe II
742.228	133.258	0	0	Ni I
744.697	0	189.887	0	S I
751.086	0	0	124.719	Fe II
753.207	0	151.275	0	Ru I
757.826	0	148.168	0	Ti III
768.845	138.651	0	0	Fe II
773.470	194.831	0	0	Hg I
775.597	0	151.275	0	Gd I
777.728	133.258	0	0	Cs II
784.482	0	170.359	0	Sm II
786.604	0	0	138.651	Ce I
797.619	0	126.421	0	Ti I
799.743	0	0	135.955	Cs II
802.23	0	131.747	0	Hg I
810.740	0	0	113.483	Fe II
815.375	0	137.516	135.955	Br I
819.648	0	123.314	130.561	C III
824.251	135.955	0	0	Fe I
828.549	138.651	0	0	Fe II
835.282	151.275	149.887	127.865	Fe II
839.568	0	178.792	0	Pb II
844.179	133.258	0	0	S II
848.444	0	0	133.258	Ne I
857.296	164.269	0	0	Pa I
859.726	0	0	127.865	Pu I
861.934	175.056	0	0	Kr II
864.059	0	167.696	0	W I
870.780	141.797	195.213	0	Sr III
872.914	0	0	158.426	Fe I
877.186	0	148.168	0	Ar II
879.666	0	0	166.966	Ne II

3.2.4 Tooth No. 4:

Figures (3-4a), (3-4b) and (3-4c) show the LIBS spectra of teeth No.4 (the healthy , edge and caries regions respectively).

Table (3-4) list the analysis of these spectra and the comparison between them.

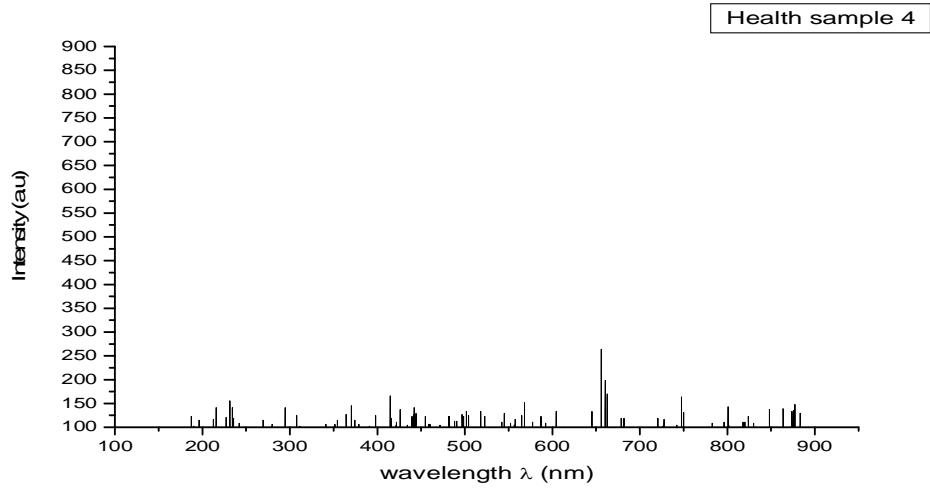


Fig. (3.4a) LIBS emission spectrum of tooth No. 4 (health region)

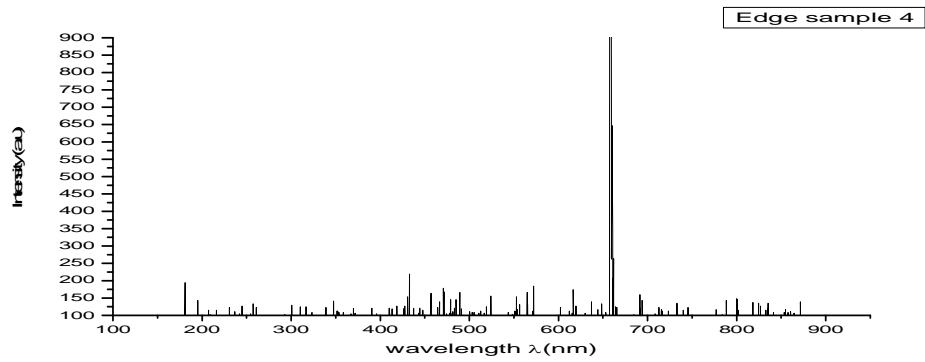


Fig. (3.4b) LIBS emission spectrum of tooth No. 4 (edge region)

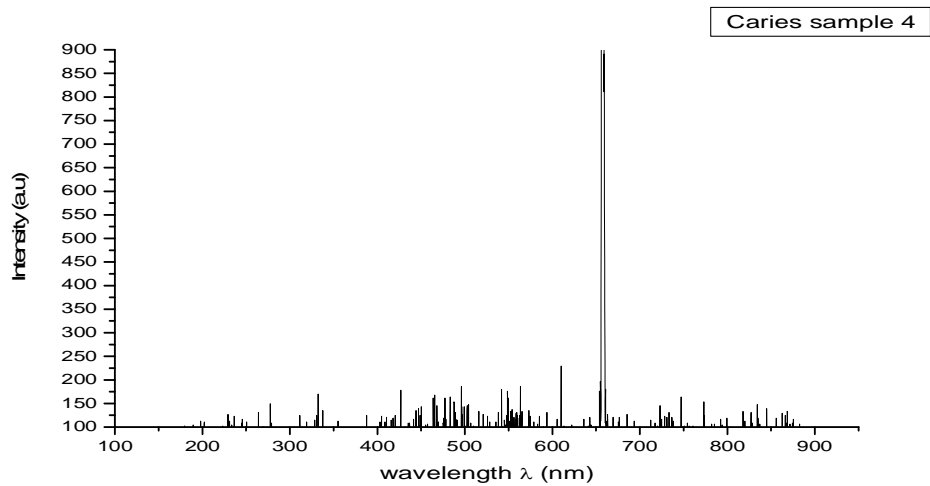


Fig. (3.4c) LIBS emission spectrum of tooth No. 4 (caries region)

Table (3.4): analysis of LIBS emission spectrum for tooth No 4 (health, edge and caries)

Recorded wavelength λ (nm)	Health	Edge	Caries	Elements and ions
	Intensity (a.u)	Intensity (a.u)	Intensity (a.u)	
186.668	144.494	0	0	Cs II
188.799	0	0	116.629	Fe II
195.193	0	160.674	0	Au I
195.547	130.561	0	0	Co II
197.326	0	0	122.022	Ti II
201.586	0	0	119.325	Al II
205.850	0	128.314	0	Sc I
215.444	155.73	0	0	Fe I
216.508	0	128.314	0	Cs II
222.900	0	0	116.629	Na VII
226.454	144.494	0	0	Ne IV
229.297	0	0	135.505	Ar III
231.072	169.662	0	0	Ne II
231.424	0	136.404	0	Kr II
235.687	0	0	132.808	Fe II
237.817	0	125.617	0	Co II
242.080	135.955	0	0	Rb III
244.213	0	141.797	0	Fe II
246.343	0	0	127.415	Ti II
250.604	0	0	124.719	W II
256.998	0	149.887	0	W I
263.395	0	0	140.898	Al I
268.722	135.955	0	0	Hf III
278.311	0	0	165.168	Er III
279.735	130.561	0	0	Hg II
293.230	0	117.528	0	Mn II
295.369	149.887	0	0	Fe I
299.623	0	144.494	0	Cs III
308.503	138.651	0	0	Ti I
310.277	0	139.101	140.898	Na II
316.674	0	139.101	0	W I
318.803	0	0	127.415	Tb II
323.068	0	122.921	0	Kr I
333.723	0	0	178.651	Ho II
337.983	0	0	151.685	Cr II

340.117	0	136.404	0	Os I
341.528	124.719	0	0	W I
348.655	0	157.977	0	Fe I
355.036	138.651	0	130.112	Si III
359.297	0	122.921	0	W I
363.914	144.494	0	0	Mn I
365.690	0	120.224	0	Os I
369.954	0	136.404	0	Ne II
370.307	155.73	0	0	Sr I
374.930	133.258	0	0	Be II
379.187	122.022	0	0	Dy II
389.130	0	0	140.898	Nb I
390.552	110.786	0	0	Si I
391.262	0	136.404	0	Sr IV
395.521	0	120.224	0	K II
396.949	135.955	0	0	Fe III
404.051	0	0	138.202	Sc III
410.446	0	0	138.202	Fe I
414.704	180.898	0	0	Cl II
416.840	0	0	135.505	Ac II
418.973	0	141.797	0	Al III
421.114	0	0	140.898	Rh I
421.444	133.258	0	0	Ru I
425.361	0	0	192.134	Gd II
425.718	141.797	0	0	Ne II
431.765	0	236179	0	W I
434.603	119.325	0	0	Ne I
436.016	0	136.404	122.022	Tb I
441.356	153.033	0	0	Ne I
448.809	0	128.314	0	Ne I
450.945	0	0	159.775	Am II
454.496	135.955	0	0	Ce II
455.195	0	0	119.325	Ta I
457.333	0	179.55	0	Kr II
459.110	119.325	0	0	Ru I
465.857	0	155.28	181.348	Be IV
470.128	0	193.033	0	Sc I
472.252	122.022	0	0	Bi I
476.522	0	0	175.955	Cl II
478.649	0	160.674	0	K I
481.134	138.651	0	0	Nd II

482.910	0	0	178.651	Fe II
485.038	0	160.674	0	Mg III
487.188	0	0	167.865	W I
489.305	0	182.247	0	Ti I
490.012	133.258	0	0	Y II
495.698	0	0	202.921	Co II
496.768	147.191	0	0	W I
501.025	147.191	0	0	W II
502.084	0	125.617	0	Sc I
504.218	0	0	162.471	Ni I
508.492	0	0	124.719	N III
512.741	0	128.314	0	Er II
517	0	0	148.988	Be III
518.785	141.797	0	0	Ho I
519.137	0	139.101	0	Xe II
521.271	0	0	143.595	Co I
523.041	135.955	0	0	F I
523.402	0	171.46	0	Ne I
525.532	0	0	138.202	Mn I
540.447	0	0	194.831	Hf I
542.591	0	122.921	0	P II
545.427	147.191	0	0	Er II
546.840	0	0	189.438	Sc I
551.108	0	168.764	0	Fe II
551.816	119.325	0	0	Ba III
555.360	0	144.494	0	Sc I
556.437	116.629	0	0	N I
559.620	0	0	146.292	Sn II
563.880	0	0	202.921	Tb I
566.021	0	182.247	0	Os I
567.447	164.269	0	0	Mo I
572.412	0	198.426	0	Sc I
574.553	0	0	151.685	Dy I
576.340	124.719	0	0	W I
578.815	0	0	127.415	Ce I
585.208	0	0	138.202	Br I
587.321	138.651	0	0	Fe I
591.966	122.022	0	0	W I
593.730	0	0	146.292	Ti II
602.256	0	136.404	0	Er I
604.398	0	0	132.808	Cs III

605.088	141.797	0	0	Pr I
608.654	0	0	243.37	N II
610.779	0	128.314	0	Ti II
615.038	0	0	116.629	Cu II
617.177	0	190.337	0	Kr II
621.441	0	141.797	0	N I
623.556	0	0	119.325	Sc II
629.966	0	120.224	0	Zr I
636.362	155.28	132.808	0	Pr II
642.770	0	0	138.202	W I
644.879	149.887	131.011	0	Kr I
649.150	0	147.191	0	W I
653.403	0	122.921	0	W I
655.887	276.179	0	0	Th I
668.328	0	0	138.202	Re I
676.836	0	0	138.202	O III
678.278	130.561	0	0	W I
682.544	130.561	0	0	Er I
685.374	0	117.528	143.595	W I
691.793	0	174.157	0	Al II
693.876	0	0	130.112	K I
708.830	0	120.224	0	Sm I
710.934	0	0	130.112	W I
713.092	0	136.404	0	Fe I
717.338	0	0	124.719	W I
720.189	130.561	0	0	Ce I
721.601	0	128.314	159.775	C I
726.910	130.561	0	0	Hg I
734.394	0	152.584	146.292	Ne II
740.782	0	128.314	0	O II
742.228	113.483	0	0	Ni I
745.045	0	136.404	0	Ti III
746.822	175.056	0	0	W I
747.172	0	0	178.651	Fe II
753.577	0	0	124.719	Ne I
772.761	0	0	167.865	Ni I
777.106	0	131.011	0	Sc I
781.275	0	0	119.325	Sm II
781.967	119.325	0	0	W I
789.846	0	160.674	0	Ca III
794.092	0	0	132.808	W I

795.493	113.483	0	0	Fe I
799.743	149.887	0	0	Cs II
800.481	0	163.37	135.505	Ca III
817.502	122.022	152.584	148.988	W I
823.904	0	152.584	0	Sc I
824.251	124.719	0	0	Fe I
826.068	0	0	146.292	W I
831.006	122.022	0	0	Fe I
834.554	0	152.584	162.471	H I
840.944	0	122.921	0	W I
845.216	0	0	154.382	S I
848.444	144.494	0	0	Ne I
855.936	0	131.011	135.505	Xe I
862.250	0	0	146.292	Ti I
864.059	144.494	0	0	W I
864.343	0	120.224	0	Nd II
868.640	0	0	148.988	W I
870.780	0	155.28	0	Sr III
875.046	0	0	132.808	H I
877.186	158.426	0	0	Ar II
881.451	0	0	119.325	Fe II
883.963	138.651	0	0	La I

3.2.5 Tooth No. 5:

Figures (3-5a), (3-5b) and (3-5c) show the LIBS spectra of teeth No.5 (the health , edge and caries regions , respectively).

Table (3-5) list the analysis of these spectra and the comparison between them.

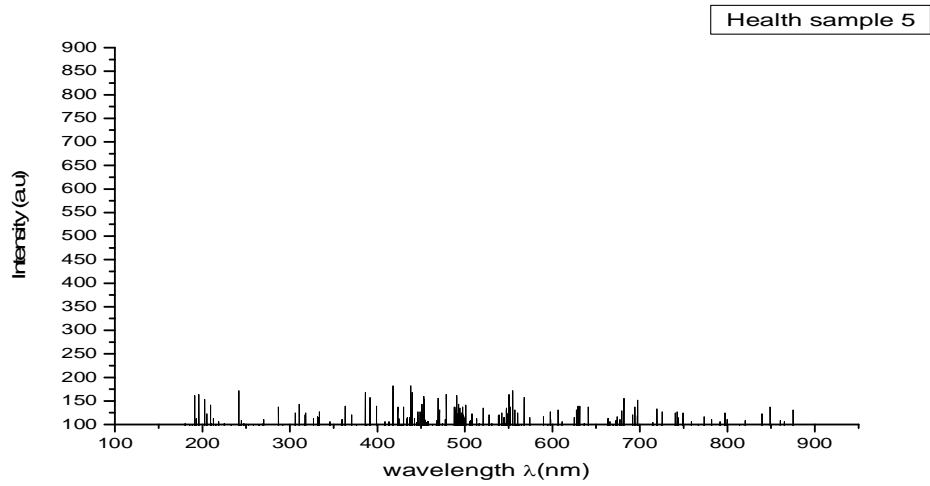


Fig. (3.5a) LIBS emission spectrum of tooth No. 5 (health region)

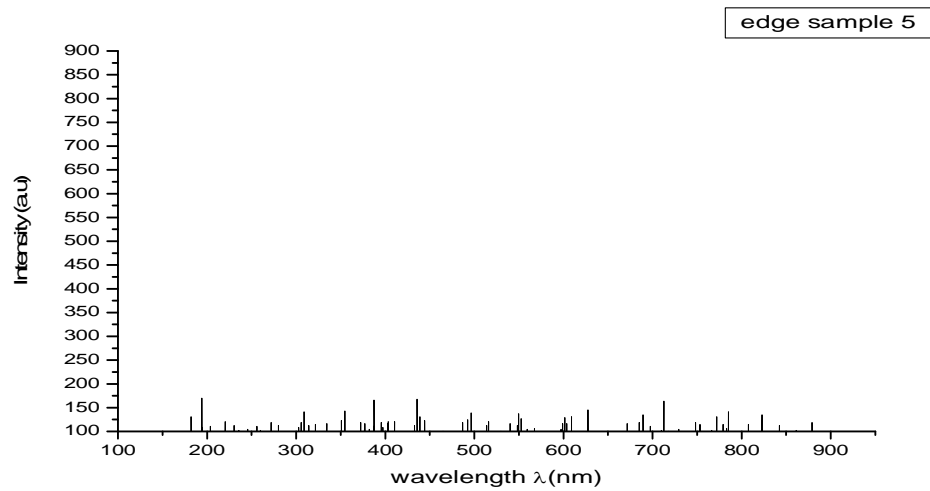


Fig. (3.5b) LIBS emission spectrum of tooth No. 5 (edge region)

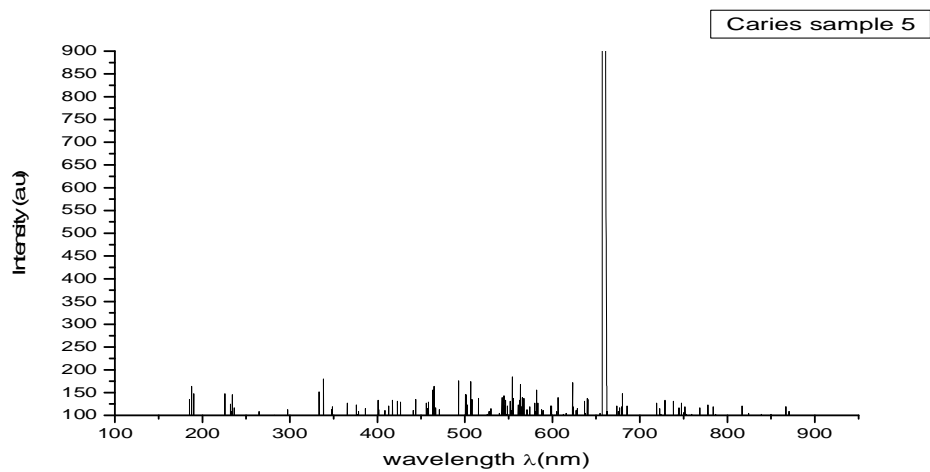


Fig. (3.5c) LIBS emission spectrum of tooth No. 5 (caries region)

Table (3.5): analysis of LIBS emission spectrum for tooth No 5 (health, edge and caries)

Recorded wavelength λ (nm)	Health	Edge	Caries	Elements and ions
	Intensity (a.u)	Intensity (a.u)	Intensity (a.u)	
182.408	0	144.943	0	Sc I
186.668	0	0	178.202	Cs II
190.936	0	0	162.022	W II
191.286	175.505	0	0	Cl III
193.063	0	185.393	0	Yb III
195.535	178.202	0	0	S II
201.921	167.415	0	0	Na II
203.716	0	126.067	0	Sr III
208.335	156.629	0	0	Fe II
212.597	129.662	0	0	S II
216.858	121.573	0	0	W II
220.764	0	136.853	0	Ta IV
225.385	118.876	0	0	Co II
227.167	0	0	162.022	Co II
231.424	0	128.764	0	Kr II
233.556	0	0	159.325	Fe II
235.687	0	117.977	0	Fe II
242.432	188.988	0	0	IR II
246.343	0	120.674	0	Ti II
254.868	0	126.067	0	Ce II
259.130	0	117.977	0	La IV
263.397	0	0	124.269	Fe II
269.786	0	134.157	0	Co II
270.142	126.966	0	0	Mo II
280.443	0	128.764	0	Hg I
287.189	151.235	0	0	W II
297.494	0	0	129.662	Ti I
301.756	0	123.37	0	Yb II
306.372	140.449	0	0	Xe II
308.148	0	155.73	0	Cd II
310.634	159.325	0	0	Xe III
314.542	0	128.764	0	Ne II
317.020	140.449	0	0	W I
320.935	0	128.764	0	Ne II
325.551	129.662	0	0	W II

331.945	143.146	0	0	W II
333.723	0	0	167.415	Ho II
335.853	0	131.46	0	Ar III
337.983	0	0	197.078	Cr II
346.852	121.573	0	0	Mn II
348.655	0	0	135.056	Fe I
350.777	0	136.853	0	Co II
355.036	0	161.123	0	Si III
359.650	126.966	0	0	Ti II
363.914	153.932	0	0	Mn I
365.690	0	0	143.146	Os I
370.307	137.752	0	0	Sr I
372.080	0	134.157	0	Xe II
374.214	0	0	137.752	Fe I
376.347	0	131.46	0	Nd II
378.473	0	0	124.269	Nd II
380.612	0	120.674	0	C III
384.873	0	0	129.662	Tb II
385.222	180.898	0	0	Cr I
389.138	0	182.696	0	Nb I
391.624	172.808	0	0	Cr I
395.530	0	134.157	0	W I
400.144	153.932	0	0	Cr I
401.922	0	0	148.539	W I
404.051	0	136.853	0	Sc III
408.318	0	0	126.966	P V
408.666	121.573	0	0	Sc I
410.446	0	136.853	0	Fe I
412.572	0	0	137.752	W I
412.933	121.573	0	0	O II
416.840	0	0	148.539	Ac II
417.193	197.078	0	0	Na II
423.235	0	0	145.842	Ti I
423.589	151.235	0	0	Fe I
429.962	151.235	0	0	Ti I
433.875	0	182.696	0	Os I
438.152	0	144.943	0	Kr II
438.505	197.078	0	0	Ne II
442.418	0	0	151.235	Fe I
451.296	172.808	0	0	Tb II
459.469	0	0	145.842	Sc I

465.857	0	0	178.202	Be IV
470.128	0	0	129.662	Sc I
470.474	170.112	0	0	Cs II
479.001	178.202	0	0	Na VI
487.188	0	134.157	0	W I
489.657	175.505	0	0	N III
491.433	0	139.55	191.685	W I
495.698	0	153.033	0	Co II
500.317	156.629	0	0	Co II
502.084	0	0	159.325	Sc I
506.704	137.752	0	0	N V
508.477	0	0	191.685	Fe III
517	0	136.853	0	Be III
517.010	0	0	151.235	Fe II
521.627	151.235	0	0	Fe I
528.014	137.752	0	0	Hg II
529.796	0	0	129.662	Cr I
538.688	137.752	0	0	P II
540.447	0	131.46	0	Hf I
542.942	140.449	0	0	Sc I
544.712	0	0	159.325	Ne I
548.987	0	150.337	0	Ti I
549.332	178.202	0	0	Fe I
553.230	0	0	199.775	Zr I
553.586	188.988	0	0	Ba I
559.620	0	120.674	0	Sn II
559.980	140.449	0	0	Eu I
563.88	0	0	180.898	Tb I
566.385	172.808	0	0	Xe III
568.150	0	120.674	0	Fe I
574.553	0	0	135.056	Dy I
574.902	129.662	0	0	Kr I
583.078	0	0	170.112	Br II
587.321	0	0	129.662	Fe I
589.821	132.359	0	0	Fe I
597.973	0	0	137.752	Pm I
598.340	143.146	0	0	Ce II
600.118	0	144.943	0	Al II
606.509	0	0	153.932	Tc I
606.874	145.842	0	0	Ti II
608.654	0	144.943	0	N II

611.149	118.876	0	0	Cd I
617.177	0	0	121.573	Kr II
623.556	0	0	188.988	Sc II
627.833	0	161.123	0	Ta I
629.966	0	0	129.662	Zr I
634.572	153.932	0	0	Sr I
636.341	0	0	145.842	Ru I
640.619	0	0	151.235	Te I
640.974	151.235	0	0	Ne I
664.413	129.662	0	0	Cu III
670.452	0	131.46	0	Ce II
672.957	132.359	0	0	Ce I
674.710	0	0	137.752	Hg I
681.102	0	0	162.022	Ti I
681.474	170.112	0	0	Fe I
685.374	0	134.157	137.752	W I
689.637	0	150.337	0	Tb II
694.252	151.235	0	0	Mn I
698.188	0	126.067	0	W I
698.515	167.415	0	0	Yb III
708.830	0	117.977	0	Sm I
713.057	0	180	0	Ti I
715.540	121.573	0	0	Er II
719.481	0	0	143.146	Eu II
719.832	148.539	0	0	Sc I
724.090	143.146	0	0	Sm II
727.995	0	120.674	148.539	Cs I
738.656	0	0	145.842	W I
741.139	140.449	0	0	Zr I
747.172	0	0	143.146	Fe II
749.308	0	134.157	0	W I
749.669	140.449	0	0	Fe II
751.444	0	0	135.056	Nd II
753.577	0	128.764	0	Ne I
758.193	121.573	0	0	W I
766.352	0	117.977	0	Nd II
768.445	0	0	132.359	Tc I
770.616	0	144.943	0	Tb II
773.103	132.359	0	0	FeII
779.143	0	128.764	0	Na III
781.632	126.966	0	0	Zr I

783.409	0	155.73	135.056	P I
790.146	121.573	0	0	S I
796.545	140.449	0	0	Tc I
806.846	0	128.764	0	Sm II
817.502	0	0	137.752	W I
819.917	124.269	0	0	Ti II
821.771	0	150.337	0	Pb I
823.904	0	0	121.573	Sc I
838.800	0	0	118.876	Bi II
839.169	137.752	0	0	Ge I
840.944	0	128.764	0	W I
847.704	151.235	0	0	Fe II
860.463	124.269	0	0	Te II
862.250	0	117.977	0	Ti I
864.766	121.573	0	0	Ce I
866.548	0	0	135.056	Th I
870.780	0	0	124.269	Sr III
875.400	145.842	0	0	Ar II
879.311	0	134.157	0	Na I

3.3 Discussion

The fifteen spectra of samples show the essential atoms Ca, P, O, and H (formed the hydroxyapatite $\text{Ca}_{10}(\text{PO}_4)(\text{OH})_2$) with different amounts for each sample. There were also common relatively small amounts of other elements, including (Fe and W) found in all the five samples with different amounts as presented in the five tables (3.1), (3,2), (3,3), (3,4) and (3.5), respectively.

The Iron was found with a large amount in sample 1, 3 in the health case and start to decrease in edge case and more decrease in caries region and sometime disappeared while in samples 2,4 and 5 it appeared in varying degrees. Also Tungsten was found in large amounts in sample 5 while it appeared in varying degrees in samples 1,2,3 and 4. This appearance of Tungsten is due to the contribution of

the background of laser lamp intensity that was not stored due to the change in its intensity. Although Calcium (Ca^+) is an important element in tooth but it appeared in sample 3 in health case only while in sample 4 in edge case and decrease in caries case while they didn't appear in the other samples.

In sample 1 there are some elements that didn't appeared in health case but start to appear in edge with certain amount and then increased in caries case like Thorium (Th), Cerium (Ce), Ytterbium (Yb), Fluorine (F). The appearance of these elements is a sign of caries formation.

Also There are some elements that appeared in sample 2 with certain amount in health case then this amount was decreased in edge case and disappeared in caries and this refers that they are decreased gradually due to caries. These elements are Manganese (Mn) and Terbium (Tb). In Addition to that, the Praseodymium (pr II) ions are appeared in sample 1,3 and 4 and didn't appeared in sample 2 and 5 . In 1,3 and 4 appeared with a certain amount in health case and decrease in edge case while they disappeared in the caries case and this is referred to the caries formation .

There were relatively small amounts of neutral atoms which are not common for the five samples including (Be , Sc, Sr, Th, Ti, Mn, Mo, Rb, Tb, Y, Eu, Kr, Gd, Cl, Gd, Ru, Xe, V, Cs, Ne, Si, Na, Ne, Dy, Zr, Sm, Sc, He and Nd), and this is may be due to the relative difference in the structure of the teeth.

3.4 Conclusions

From the experimental results obtained in this work one can conclude that

- The LIBS technique detected the essential atoms Ca, H, O forming the structure of the samples (the hydroxyapatite $\text{Ca}_{10}(\text{PO}_4)(\text{OH})_2$) with different amounts for each sample of the five teeth. Other elements that are not essential (like Fe, Hg, Kr, Nb, Ne, Ru, Sc, Sr, and w) were appeared with different amounts in all five samples .
- A spectroscopic change happen in sample 1 where some elements didn't appeared in health case but start to appear in edge with certain amount and then increased in caries case, like Thorium (Th), Cerium (Ce), Ytterbium (Yb), Fluorine (F). The appearance of these elements is a sign of caries formation.

In Addition to that, the Praseodymium (pr II) ions are appeared with a certain amount in health case and decrease in edge case while they disappeared in the caries case and this is referred to the caries formation .

- In sample 2 the spectroscopic change that happen was indicated for some elements and ions that appeared in health case but start to decrease in edge with certain amount and then disappeared in caries case, like Terbium (Tb) and Manganese (MnII), Cerium (CeII) ions The appearance of these elements is also a sign of caries formation.

Also the ions like Zirconium (ZrIII), Gadolinium (GdII), Yttrium (YII), and Cerium (CeIII) were appeared in health case with a certain amount and decrease in edge and more decrease in caries case while the Titanium (Ti) element was disappeared in health

case but appeared in edge and decrease in caries case for the same reason.

- In sample 3 the change is that some elements are appeared with a certain amount in health case and decrease in edge case while they disappeared in the caries case like the Praseodymium (Pr II), Neon (NeII) ions and iron (Fe), Strontium (Sr), Xenon (Xe). There are other elements and ions like (FeII),(Fe) are appeared in health case and decrease in edge case with more decrease in caries case and this is referred to the caries formation also .

There are some elements and ions like Bismuth (Bi), Krypton (Kr), Chlorine (ClIII) were disappeared in health case while appeared in edge case and increase in caries case.

Also the elements like, Zirconium (ZrI), Dysprosium (DyI), Bromine (BrI) and the ion of Chlorine (ClIII) were disappeared in health case also while appeared in edge case and decrease in caries case.

- The spectroscopic change that happen in sample 4 is that some elements and ions didn't appear in health case but start to appeared in edge with certain amount and then decreased in caries case like Iron ion (FeII), Terbium (Tb), Neon (NeII), Calcium ion (CaIII). Some elements and ions were disappeared in health case while appeared in edge case and increase in caries case like Sodium (NaII), Beryllium (BeIV), Chlorine (Cl), Hydrogen (H). Others elements and ions like Krypton (Kr), Praseodymium (PrII) were appeared in health and decrease in edge while it disappeared in caries. The appearance of these elements is a sign of caries formation.

- The change that happen in sample 5 is that the Cesium (Cs) was disappeared in health case while appeared in edge case and increase in caries case. All the changes that happen in the five samples with three cases cleared that each sample have a certain amount of elements that differ from others specially in case of caries. There are some elements that were disappeared and other were appeared depend on the structure of the tooth itself.
- LIBS is a good diagnostic technique for dental caries in teeth samples.

3.5 Future work

From the results, the followings can be suggested as future work:

1. Study a lot of teeth to specify exactly the change that happen due to caries.
2. Diode pumped Nd YAG laser can be used to overcome the pumping lamp background .
3. Double pulse laser systems can be used to enhance the detected signal.

REFERENCES

1. **Solarz, R. W. & J. A. Paisner.** (1986). *Laser spectroscopy and its application*, New Mexico state university. las cruces, New Mexico & Richard W, Taylor & Francis.
2. **Sune Svanberg.** (2004). *Atomic and Molecular spectroscopy*, 4th Ed. Berlin/DE. Springer - Verlag Berlin & Heidelberg Gmbh & Co. K.
3. **DR. H. Kaur** (2009) *spectroscopy*, US, (Senior lecturer postgraduate department of chemistry).
4. **Jerry workman, Art Springsteen** (1998) *Applied spectroscopy*, San Diego/US, Elsevier Science Publishing Co. Inc.
5. **Orazio Svelto** (2012) *Principles of lasers*, fifth edition, Softcover Reprint of the origin ed. NewYork/US, Springer – Verlag NewYork Inc.
6. **K.R. Nambiar** (2009), *Lasers principles, types and applications*, New Dehli/In, New age international Pvt Ltd publishers.
7. **Grant R. Fowles** (2009) *Introduction To Modern Optics* Second new edition, NewYork/US, Dover publications Inc.
8. **Frank Trager** (2007) *Handbook of lasers and Optics*, NewYork/US, springer – verlag NewYork Inc.
9. **William T. Silfvast** (2008) *Laser Fundamentals*, second revised, Cambridge/GB, CAMBRIDGE UNIVERSITY PRESS.
10. **John F. Ready** (1997) *Industrial application of laser*, second edition, San Diego/US, Elsevier Science publishing Co. Inc.
11. **Wolfgang Demtroder** (2002) *Laser Spectroscopy – Basic concepts and instrumentation*, third edition , Berlin/DE, springer – verlag Berlin and Heidelberg Gmbh & Co. KG.

12. **Marco J. Castaldi, Selim M. Senkan** (1998) *Real - Time, Ultrasensitive Monitoring of Air Toxics by Laser Photoionization Time – of – flight mass Spectrometry*. Journal of the Air & waste Management Association,48(1): 77 – 81.
13. **Z. Dai, L.K. Tseng, & G.M. Faeth**, (1995) *Velocity/ mixture fraction statistics of round, self- preserving, buoyant turbulent plumes*. Journal of heat transfer transactions of the ASME. 117:918-26.
14. **Sanders, S.J., Boivin, R.F., Bellan, P.M., Stern. R. A.** (1999) *Added discussion of 'Observations of fast anisotropic ion heating, ion cooling, and ion recycling in large-amplitude drift waves'*, phys. Plasmas. 6,4118.
15. **Maslov, D.V. Fadeev, V.V. & Lyashenko A.I.** (2000) *A Shore - Based Lidar for Coastal Seawater Monitoring*. EARSeI-SIG-Workshop LIDAR, pag. 46-52.
16. **J. Michael Hollas** (2004) *Modern spectroscopy*, fourth edition, chichester/GB, John Wiley & Sons Ltd.
17. **Celio Pasquini, Juliana Cortez, Lucas M. C. Silva, Fabiano B. Gonzaga** (2007) *Laser Induced Breakdown Spectroscopy*. Journal of Braz. Chem.Soc. 18, 463-512.
18. **Scaffidi J, Angel S.M, Cremers, D.A.** (2006) *Emission Enhancement Mechanisms in Dual-Pulse LIBS*. Analytical Chemistry, 78(1): 24 – 32. PubMed PMID:16419334.
19. **Cengiz, S, et al** (2004) *SEM-EDS Analysis and Discrimination of Forensic Soil*. Forensic Science International. 141, 33-37.
20. **B. T. Fisher, H. A. Johnsen, S. G. Buckley and D. W. Hahn** (2001) *Application Spectroscopy*.

21. **L. Moenke-Blankenburg** (1989) *Laser Micro Analysis*, NewYork/US, John Wiley & Son Ltd.
22. **Markolf H. Niemz** (2007) *Laser-Tissue Interactions*, third revised, Berlin/DE, Springer – Verlag Berlin & Heidelberg GmbH & Co. KG.